THE LUMINOSITY CURVE OF THE AURORAE

BY *LEIV HARANG*

(Manuscript received 16th September 1944.)

1. Introduction.

The problem of calculating the light emission or *luminosity curve* of the aurorae presupposes a knowledge of the absorption of the electrically charged particles penetrating the atmosphere. The problem of the absorption of corpuscular rays in the upper atmosphere — either electrons or positive rays — had been the subject of considerable discussion since Lenard's first paper on the absorption of cathode rays in the atmosphere. *Lenard*[1] treated the case of absorption of a cathode ray bundle penetrating rectilinearly into an atmosphere with exponential decrease of density with height. Now the orbit of an electrically charged particle will be strongly influenced by the earth's magnetic field. If the lines of force converge slightly, as in the upper region of the atmosphere, the field may be regarded as approximately equivalent to the field of a single magnetic pole.[2] According to a well-known theorem of Poincaré an electrically charged particle will in this case move along a geodetic line on a cone of revolution with the top lying in the magnetic pole. The opening of the cone and the position of the geodetic line will depend on the velocity of the particle and the angle ψ between the field of force and the orbit of the particle when the latter is entering the earth's magnetic field. The orbits of a bundle of electrically charged particles forming an isolated auroral ray or the bundle of rays constituting a drapery or drapery-shaped arc will therefore, be spirals in which the density and the width of the windings are unknown. Fig. 1[3] illustrates different examples of possible orbits, *a* being the orbit of a single particle, *b* of particles with different angles ψ, and *c* of a particle with a small value of ψ, thus approaching the rectilinear example.

It is evident that the region of absorption, and even more the distribution of the auroral luminosity, will be strongly influenced by the shape of the corpuscular orbit and the number of windings around the field of force. If we assume that the ray bundle is deflected back without appreciable absorption, the height and the luminosity curve of the aurorae will be mainly determined by the shape of the orbits.

Regarding the type of spirals constituting the orbits, different opions have been expressed. *Birkeland*[4] was of the opinion that the rotation of the orbits was negligible, the orbits thus approaching the rectilinear example demonsrated in Fig. 1 *c*. The orbits with backward reflection were rejected.

Birkeland based his view mainly on the results obtained by his terrella experiments. Størmer has adopted no definite standpoint as to the effects of the spiral nature of the orbits on the absorption and luminosity distribution in the aurorae. In a later paper, *Størmer*[5] has extended Lenard's calculation of the absorption of cathode rays when taking into account the spiral nature of the orbits. The curves of absorption were calculated numerically for a

[1] *Lenard:* Über die Absorption der Nordlichtstrahlen in der Erdatmosphäre. Heid.Sitzungsber. Ak. Wiss., Abh. 12 (1911).

[2] *Vegard:* Recent Results of Northlight Investigations etc. Phil. Mag. *42*, 47 (1921) and Størmer: Rapport sur une expédition d'aurores boréales à Bossekop et Store Korsnes pendant l'année 1913. Geofys. Publ. *1*, No. 5 (1921) § 29, 165—169.

[3] The orbits are taken from *Størmer's* Geneva paper of 1911: Sur les trajectoires des corpuscles électrisés dans l'espace etc. Archives des science physique et naturelles *32*, 1—163 (1912), p. 127 and 128.

[4] Cited in *Størmer's* paper, footnote 3, p. 128—129.

[5] *Størmer:* Rapport d'une expédition d'aurores boréales à Bossekop et Store Korsnes pendant le printemps de l'année 1913. Geofys. Publ. *1*, No. 5 (1921),p. 187.

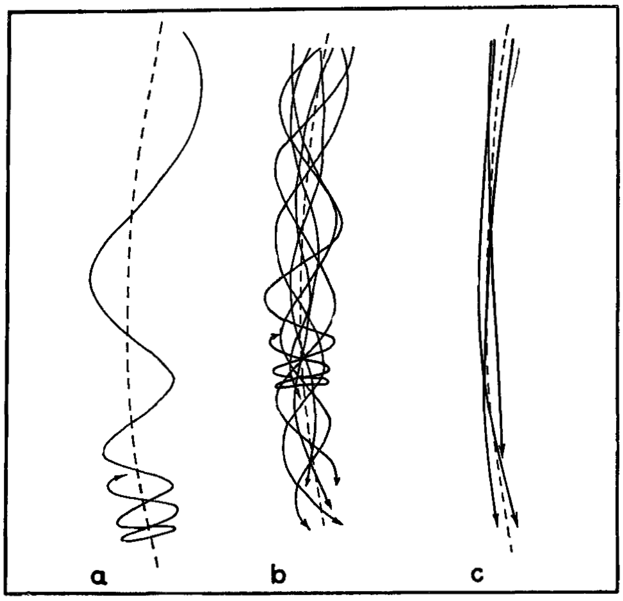

Fig. 1.

bundle of cathode rays of stiffnes $H\varrho = 700$ entering a model atmosphere under varying angles of ψ in the interval 0—90°. Størmer's numerical calculations for this special show that the spiral nature of the orbits has little influence on the absorption for values of ψ lying in the interval 0—60°. It would be of great interest to have these numerical calculations extended to series of cathode rays with other velocities penetrating into different model atmospheres.

Vegard[6] has strongly advocated the view that the spiral nature of the orbits plays a decisive role in causing the absorption and luminosity distribution in the aurorae. According to Vegard the height of the lower borders and especially the light distribution the rays and draperies are mainly determined by the spiral nature and the partially backward-deflected orbits.

A theoretical and experimental study of the luminosity distribution in the aurorae was first made by *Vegard*[7]. Assuming that the light emission L produced by the absorption of a bundle of cathode rays is proportional to the rate of absorption, dS/dh, where S is the intensity of the cathode ray in the height h, we can determine the luminosity curve from Lenard's absorption curves, for instance by graphical derivation. We have here regarded the simple case of cathode rays penetrating the atmosphere vertically downwards.

For positive rays the construction of the luminosity is more complicated. *Vegard*[7] here uses the experimentally determined curve of ionisation for a positive ray bundle penetrating the air. Assuming that the luminosity produced is proportional to the ionisation produced along the ray bundle, it is possible to construct a luminosity curve for a bundle of positive rays penetrating an atmosphere. As the ionisation curve of positive rays has a steep maximum just before the maximum range of the particles, the luminosity curve produced by positive particles will exhibit a steep maximum just above the lower boundary of the aurorae, — assuming rectilinear paths for the particles in this case also.[8]

From auroral photos taken at the Haldde observatory in 1914 *Vegard*[9] has estimated the dimensions of the auroral luminosity. The distance l_1 from the bottom edge to the point of maximum luminosity, the distance l_2 from the bottom edge to the limit of the strong luminosity and the distance l_3 from

* Professor *Vegard* kindly pointed out to the author that the application of the simple exponential formula hitherto used for calculating the absorption (and thus also the luminosity) of a bundle of cathode rays penetrating a gas, is subject to to certain limitations. The use of the exponential formula presupposes that the absorption of the cathode rays in a homogeneous medium is a parallel to the absorption of light or X-rays. For cathode rays, however, the exponential formula is only valid when the electrons are scattered during the passage. The orbits of the ***individual*** electrons in the ray bundle will therefore ***not*** be rectilinear although the bundle as a whole may be regarded as rectilinear

The curve of ionisation (and also of light emission) of a ray bundle where the electrons move strictly parallel will be of the same type as for α-rays. When a strictly parallel ray bundle penetrates a homogeneous medium the ionisation (and light emission) will not decrease according to an exponential law, but steadily increase up to a sharp maximum just before the ray bundle is completely absorbed.

6 See footnote 2 and the article: The Aurora Polaris and the upper Atmosphere, p. 603—609, in J. A. Fleming's monograph: Terrestrial Magnetism and Electricity, N. Y. 1939.

7 *Vegard:* Über die physikalische Natur der kosmischen Strahlen, die das Nordlicht hervorrufen. Ann. d. Phys., *50*, 853—900 (1916).

8 See also, footnote 2, § 33, Fig. 34.

9 *Vegard* and *Krogness:* The Position in Space of the *Aurora polaris.* Geofys. Publ. *1*, No. 1 (1920), p. 149 —159.

the bottom edge to the limit of the feeble luminosity were measured on the plates. These distances were measured in the direction of the earth's magnetic field of force. From material including 69 pictures Vegard gives mean values of l_1, l_2, and l_3 for the different auroral forms.

In what follows the results will be given of a photographic photometric study of the luminosity of the aurorae. In presenting the experimental data the assumption has been borne in mind that the auroral luminosity is produced by a bundle of cathode rays penetrating the atmosphere rectilinearly.

2. Computation of the Luminosity Function of Cathode Rays.

The basic assumption in computing the luminosity from the absorption curve of the cathode rays is that the luminosity L produced in the height interval dh is proportional to $\frac{dS}{dh}$, where S is the intensity of the cathode rays. Now in the theory of the ionosphere there is a parallel problem which is of great importance and which has been thoroughly discussed theoretically in recent years. This is the problem of ionisation produced by the action of a monochromatic ultra violet ray penetrating the atmosphere. In two papers *Chapman*[10] has developed a number of formulas for ion production which can in part be applied to auroral problems. As the discussion of the auroral luminosity curves is in some respects parallel to the discussion of the electron densities in the E- and F_2-layers, it will be convenient to calculate the luminosity function along the same lines as the function of ion production within an ionized layers.

The density ϱ of the atmosphere at a height h is given by the barometric height formula *

$$\varrho = \varrho_0 e^{-\mathrm{mg}/_{kT}h}, \qquad (1)$$

where m is the mean molecular mass, g the acceleration of gravity k Boltzmann's constant, T the absolute temperature and h the height.

* The formula is only valid over a plane earth. Further, the variation in g with the height is neglected.

[10] *Chapman:* The Absorption and Dissociative or Ionizing Effect of Monochromatic Radiation in an Atmosphere on a Rotating Earth. Proc. Phys. Soc. *43*, 26—45 (1930) and *44*, 483—501 (1931).

In the discussion of the density formula we usually put

$$kT/_{\mathrm{mg}} = H. \qquad (2)$$

H, which is a function of the two variables T and m, has the dimension of a length, and may be interpreted as the total height of an atmosphere with constant temperature and density at all heights and with the same values as at the ground.

For the aurorae we must assume a fixed angle of incidence for the cathode rays, the rays entering the atmosphere in the direction of the lines of force of the earth's magnetic field at the place of observation. Further, the incident radiations may be of different velocities, i. e. they are not "monochromatic".

According to Lenard the absorption is proportional to the mass traversed. The absorption in a layer dh will accordingly be:

$$ds = \mu S \sec\chi \cdot \left(\varrho_0 e^{-h/H}\right) \cdot dh, \qquad (3)$$

where μ is the mass absorption coefficient, χ the complement to the earth magnetic inclination, S the intensity of the cathode ray bundle and $\varrho_0 e^{-h/H}$ the density of the air at the height h. We assume isotherm atmosphere and complete mixing for the level considered. Integrating the equation above, we obtain the absorption formula:

$$S = S_\infty e^{-\mu H \sec\chi\, e^{-h/H}} \qquad (4)$$

where S_∞ is the extra-terrestrial intensity.

We assume now that the number of light quanta L, or *luminosity*, emitted per cc is proportional to the decrease in intensity of the cathode ray bundle, $\frac{dS}{dh} \cdot \frac{1}{\sec\chi}$. From (4) we thus obtain the following formula for L:

$$L = \alpha \mu S_\infty \varrho_0\, e^{\{-h/H - \mu H \sec\chi \varrho_0 e^{-h/H}\}}, \qquad (5)$$

where α is the number of light quanta emitted by absorption of one unit of the radiation intensity S.

As in Chapman's discussion of the electron density curves, it will be conveniant to use the height of the *maximum* luminosity as a point of reference. The height h' of the maximum (for constant H and χ) is determined by $\frac{\partial L}{\partial h} = 0$, and we get:

$$e^{h'}/_H = \mu \varrho_0 H \sec\chi. \qquad (6)$$

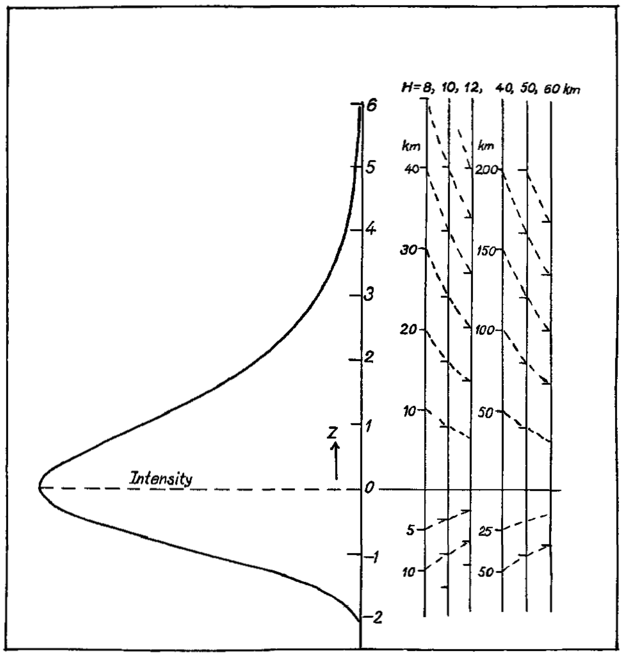

Fig. 2. Vertical luminosity curve L produced by the absorption of a bundle of cathode rays entering the atmosphere. The scale of height for various values of H is indicated to the right.

The corresponding value of L' is:

$$L' = a\, S_\infty \cos\chi \cdot \frac{1}{He}. \qquad (7)$$

Introducing the values of h' and L' in (5) we obtain:*

$$L = L'e^{\left\{\frac{h'+H-h}{H} - e^{\frac{h'-h}{H}}\right\}}. \qquad (8)$$

As in Chapman's treatment of the electron density curves, we introduce $H = kT/mg$ as a scale value of length, using a new variable z determined by the formula:

$$z = \frac{h-h'}{H}, \qquad (9)$$

and get the following simple expression of the variation of luminosity with height:

$$L = L'e^{1-z-e^{-z}}. \qquad (10)$$

Fig. 2 shows the theoretical luminosity curve. Two sets of scale values of H lying in the ranges 8—12 km and 30—70 km illustrate the vertical extensions of the luminosities for varying conditions of the upper atmosphere.

* Note: in *Chapman's* discussion the values at *equator*, *Io*, ($\chi = 0$) are introduced as the constant in the equation corresponding to (8). In equation (8), however, the constant L' corresponds to the maximum intensity at the *place of observation.*

Table 1.

		lower part			upper part		
$L/L' =$	1	$^2/_3$	$^1/_2$	$^1/_3$	$^2/_3$	$^1/_2$	$^1/_3$
$z =$	0	—0.733	—0.946	—1.190	1.058	1.461	1.953

In comparing the observations with the theoretical luminosity curve the values of $h - h'$ (in km) were determined at the points where the intensity had fallen to 66.7 %, 50 % and 33.3 % above and below the intensity maximum. The corresponding values of z from equation (10) are calculated and given in table 1.

It is thus possible to calculate H, using equation (9) with the appropriate values of z,* from the values of h—h' determined from the photometry of the aurorae.

* In his Geneva paper: Sur les trajectoires des corpuscles électrisés dans l'espace, Arch. des Sc. phys. et nat. *32*, 1—163 (1912), see p. 153—158, *Størmer* already demonstrated the possibility of a method of using the length of the auroral rays for determining the temperature of the auroral region. The method is in principle the same which has later been used in ionospheric researches for determining $H = kT/mg$, and in this paper for determining the same quantity from the luminosity curve. In Størmer's treatment of the problem he used the absorption curve of cathode rays in an atmosphere with exponential decrease of density, assuming that the temperature was constant and the molecular mass equal to that of molecular hydrogen. Assuming the length of the auroral ray to lie in the interval of absorption of the cathode rays from 0.9 I_0 to 0.1 I_0 of the initial cathode ray intensity I_0, it is possible to calculate the temperature in principally the same way as has been done in this paper. It is evident that under these assumptions the length of the auroral rays will be proportional to the temperature in the auroral region. Although the assumptions regarding the constitution of the atmosphere and the height measurements then used now have mainly historical interest, the problem of determining the quantity $H = kT/mg$ from the effects of absorption of a radiation in an atmosphere with exponential decrease of intensity was first raised by Størmer in the paper mentioned above.

3. The Material.

The material used was selected from the stock of parallactic photographs taken at the observatory and the second station at Tenness, 43 km to the south. The photographs taken during the winter 1943—44 were all furnished with a scale of intensities by using a Zeiss "Stufenfilter". The photographs taken during earlier seasons were not furnished with intensity scales. The plates being, however, of the same type and always developed in the same standard developer, the same intensity scales could be used for reducing the older material. Control tests showed that, within the limit of error, this procedure was permissible.

In selecting the photographs more than two thousand photos were examined. As a fairly big range of intensity has to be measured, it is of importance that the intensity maximum of the aurorae lies in the upper region of the linear part of the blackening curve. Almost all the photos used were of aurorae lying north and south, and only the simple fan-like forms of draperies were used. Parts of the aurorae with folds or "false rays", as indicated in Fig. 3, should be avoided.

The blackening was measured with a recording photo-electric photometer built at the observatory and previously used for filter photometry.[11] When possible the photometric trace was recorded across a reference star on the photograph. Fig. 4 shows a photometric trace of an auroral arc.

The photometric trace on the photographs was laid in the direction of the magnetic zenith. The lower and upper starting-points were marked off on the photographs, and the position of the photometric trace was drawn on the projection of the auroral photograph. The direction to the magnetic zenith was calculated for the reference stars and the deviation of the photometric trace from this direction was controlled. This deviation did not exceed 10°—12°, and a small correction on the height scale of the photometric record was sufficient to correct this inaccuracy. The formulas for determining the direction of the magnetic zenith when laying the photometric trace on the photos are given in Vegard's paper[12] and need not be repeated here.

As previously shown in the paper on filter photometry,[11] three corrections must be made in the photometric records.

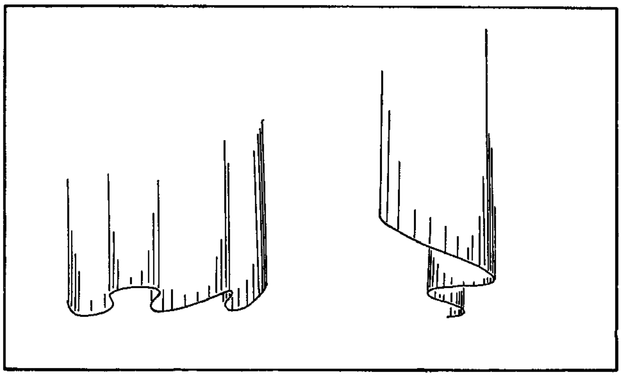

Fig. 3. Aurorae with folds and "false rays", which strongly deform the luminosity curves measured.

a. Correction for extinction. As the aurorae have an angular extension in a vertical direction the lower parts are more absorbed than the upper part, and the intensity curve thus suffers a slight deformation. The influence of extinction has been discussed in the paper mentioned. For the plates here used a coefficient of transmission of $q_\lambda = e^{-a_\lambda} = 0.750$ was used. The effect of extinction for all angular heights was calculated by Bemporad's tables.

b. Decrease of intensity in the outer field of the lens. In the case of objectives with high light power this effect may be considerable. The effect must be determined experimentally. In the paper previously mentioned this effect has been discussed and the corrections to be used are given.

For aurorae with small vertical extension, such as arcs, the corrections *a* and *b* are of minor importance. For draperies and rays they must be taken into account.

c. Correction for background fog. The most important correction is that for fog. When aurorae appear, the sky is almost always covered with a faint luminosity of varying intensity during the night. The density of this luminosity was measured in regions above and below the auroral form, and a correction was made in the photometric trace.

In Table 2 and Fig. 5. the influences of the different corrections on the photometry are demonstrated. In this case a drapery with considerable angular extension was measured, and the corrections are fairly great compared with the other cases.

[11] *Harang:* Filteraufnahmen von Polarlicht. Geofys. Publ. 10, No. 8 (1934).

[12] See footnote 9, p. 150—151.

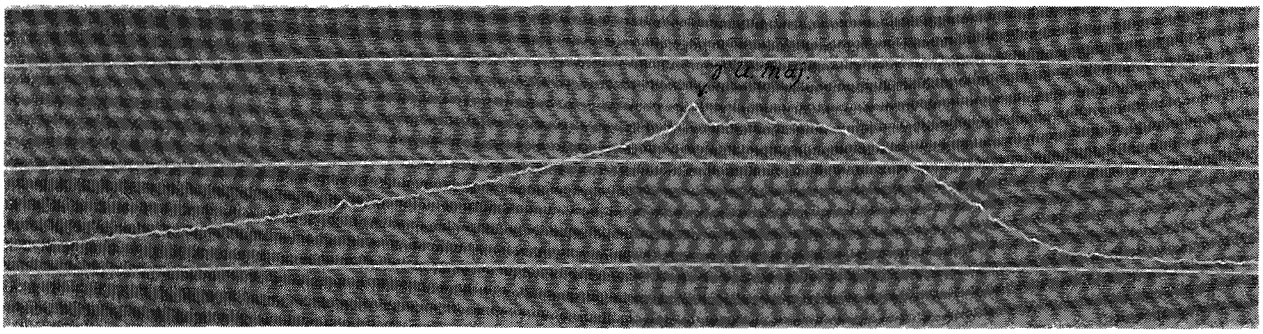

Fig. 4. Photometric record across an auroral arc.

The heights of the lower border and the extension of the draperies and rays were measured by means of parallactic photos.

4. Discussion of the Luminosity Curves.

On Plates I, II, III, and IV the luminosity curves of 54 single aurorae are demonstrated. The start and end of the photometric curves are marked with a circle, which is broken if the Tenness photo was used for photometry and continous if the Tromsø picture was used. In cases where two photometer records were laid across the auroral form, both curves of luminosities coincided within the limit of error, as in Nos. 1, 9, 10, 17, 20, 21, 25, 26, and 53, where all the points measured have been marked off and the mean luminosity curve drawn.

In order to get a survey of the results the distances in km from the luminosity maximum to the points on the lower and upper part of the intensity maximum where the luminosity has decreased to ⅔, ½, and ⅓ have been measured and tabulated in Table 3.

Table 2.

24. 10. 1935.

Point	1	2	3	4	5	Max.	6	7	8	9	10	11	12
Intensity observed, reduced for background fog.	1.6	16.2	43.5	71.6	96.7	100	96.7	85.1	61.3	35.4	20.8	11.1	2.7
Lens correction Extinction faktor.	0.78 0.370	0.84 0.386	0.88 0.402	0.92 0.418	0.96 0.434	0 97 0.441	0.97 0.450	0.98 0.465	0.98 0.497	0.96 0.530	0.90 0.561	0.82 0.592	0.68 0.625
Intensity corrected	2.4	21.4	52.5	79.5	99.0	100	94.5	79.8	53.8	29.8	17.5	9.8	2.7

26. 1. 1936.

Point	1	2	3	4	5	6	7	8	Max.	9	10	11	12	13	14	15	16
Intensity observed, reduced for background fog.	3.9	5.7	10.6	22.5	39.6	64.7	84.5	96.2	100	98.7	95.1	66.6	47.6	30.9	20.6	12.7	6.1
Lens correction Extinction factor.	1.000 0.515	1.000 0.520	0.955 0.525	0.992 0.530	0.990 0.535	0.985 0.540	0.980 0.545	0.975 0.550	0.965 0.555	0.955 0.560	0.935 0.565	0.865 0.581	0.755 0.597	0.670 0.612	0.544 0.630	0.390 0.645	0.200 0.660
Intensity corrected	4.1	5.8	10.8	22.9	40.1	64.8	84.5	98.5	100	99.0	96.3	70.6	56.2	40.3	32.1	27.0	24.6

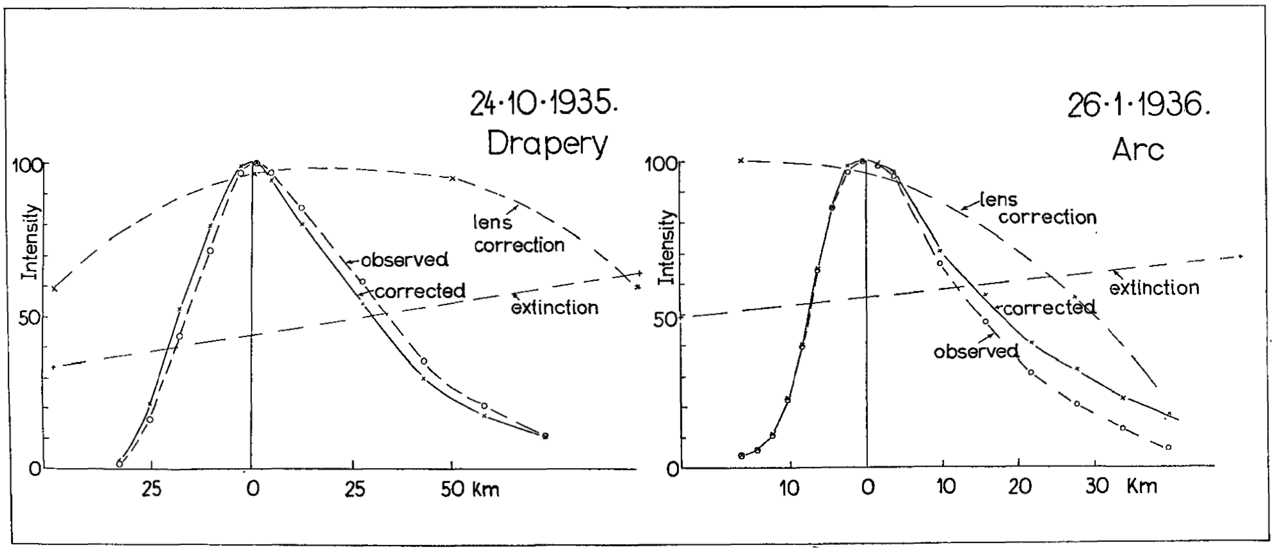

Fig. 5.

The heights h_{max} above the earth's surface of the intensity maximum determined by means of parallactic photographs are given in each case.

The luminosity curves recorded resemble the theoretical luminosity curve given in Fig. 2, a steep decrease at the lower boundary and a slighter decrease in the upper part. Further, there are points of inflection in the upper and lower parts. From Table 3 it is evident that there is an increase in the vertical extensions with increasing values of h_{max}. This is clearly seen in Fig. 6 *a* and *b*, where the values of $l_l^{2/3}$, $l_l^{1/2}$, $l_l^{1/3}$ and $l_u^{2/3}$, $l_u^{1/2}$, $l_u^{1/3}$ are arranged as functions of h_{max}.

The scattering of the l-values in Fig. 6 is considerable. This may partly be due to inaccuracies in the measurements. Further, there are reasons for assuming the existence of ebb and flood in the upper atmosphere with a maximum amplitude of 4—6 km in the displacement of h_{max} according to the hour angle of the moon.

An interesting feature is that there is a continuous increase and overlapping in the l-values from arcs with values of $h_{max} \approx$ 130—145 km to draperies with values of $h_{max} \approx$ 145—160 km. Table 4 gives the mean l-values. Below the table are given the l-values of two groups of high rays, the highest being sunlit.

We can now calculate the numerical values of $H = mg/kT$ by using the equation (9) and the corresponding numerical values of z, given in Table 1.

Table 4. Mean l-values.

h_{max}	$l_l^{2/3}$	$l_l^{1/2}$	$l_l^{1/3}$	$l_u^{2/3}$	$l_u^{1/2}$	$l_u^{1/3}$
km	km	km	km	km	km	km
100	5.3	6.8	8.2	9.2	13.5	18.6
110	5.7	7.2	8.8	10.3	15.2	20.8
120	6.7	8.8	10.1	12.1	18.4	24.7
130	8.2	11.0	12.3	14.3	22.0	29.3
140	10.3	13.4	15.3	17.2	25.5	33.8
150	13.8	18.0	22.7	21.8	30.8	41.2
160	19.6	27.6	35.0	(33.0)	(46.0)	(60.0)
185	43	53	62	46	61	79
270	76	105	135	87	117	146

In Table 5 are tabulated the H-values corresponding to $H_l = \frac{l_l^{2/3}}{0.733}$ and $H_u = \frac{l_u^{2/3}}{1.058}$. The mean values of these should give the value at the height corresponding to h_{max} for each pair.

From Table 5 it is evident that the value of H increases with the increasing height of the intensity

Table 5.

h_{max}	H_l	H_u	H_{mean}	type
km	km	km	km	
100	7.2	8.7	8.0	arcs
110	7.8	9.8	8.8	
120	9.1	11.4	10.3	and
130	11.2	13.5	12.3	
140	14.2	16.2	15.2	drape-
150	18.8	20.6	19.7	
160	26.7	(31.1)	28.3	ries
185	58	44	51	rays
270	103	88	92	sunlit rays

Table 3.

				lower part			upper part			
No.	Date	MET	h_{max}	$l_l^{2/3}$	$l_l^{1/2}$	$l_l^{1/3}$	$l_u^{2/3}$	$l_u^{1/2}$	$l_u^{1/3}$	Type
			km	km	km	km	km	km	km	
1	9. 1. 1932	21.23.00	119	6.9	8.5	10.0	13.4	18.2	24.5	arc
2		23.53	116	6.3	7.8	9.1	11.0	16.0	21.8	»
3	4. 2. »	21.17.30	100	5.8	7.2	8 9	11.4	15.9	21.7	»
4	27. 10. »	20.15.00	148	12.3	15.9	18.7				faint arce
5		16.50	146	10.9	14.0	17.5				» «
6		17.00	145	10.3	13.0	15.6				» »
7		45.25	135	7.9	9.9	12.0				» »
8		46.24	143	9.9	12.1	14.5				» »
9	22. 3. 1935	21.18.20	140	9.7	12.7	15.6	14.2	22.8	32.9	drapery
10		20.32	129	10.1	12.9	15.6	16.5	24.5	32.7	»
11	24. 10. »	17.54.00	270	67.0	95.0	125.0	73.0	102.0	136.0	sunlit rays
12		54.35	270	85.0	115.0	144.0	104.0	131.0	156.0	» »
13		21.21.30	150	13.3	18.3	22.1	19.4	30.0	40.7	drapery
14		22.28	150	14.8	18.8	22.8	22.0	34.0	47.6	«
15		34.35	145	11.7	14.9	18.1	18.0	24.3	35.5	faint arc
16		35.15	148	15.4	18.8	21.9	19 2	26.4	35.2	» »
17	27. 10. »	17.49,45	119	7.1	9.0	9.8	12.3	16.9	22.5	arc
18	5. 11. »	23.21.00	109	6.4	8.2	9.8	10.1	14.7	21.1	drapery
19		21.30	107	6.4	7.9	9.7	10.0	13.5	19.3	»
20		23.35.30	106	6.9	8.7	10.0	8.2	12.0	19.0	»
21		36.00	99	6.1	7.5	9.7	9.7	13.4	17.6	»
22	26. 1. 1936	17.18.30	110	6.0	7.5	8.8	11.7	17.0	25.0	arc
23		19.10	109	4.8	5.8	7.3	9.1	13.4	19.8	»
24		18. 6.32	110	4.7	6.0	7.1	11.2	16.0	22.7	»
25		6.48	107	4.7	5.8	6.9	10.4	16.3	22.5	»
26		7.03	108	5.2	6.5	7.6	7.9	12.5	18.8	»
27		7.16	110	5.8	7.0	8.3	10.7	14.2	19.8	»
28		7.29	108	6.4	7.9	9.2	10.6	14.8	18.9	»
29		7.40	108	5.8	7.3	8.6	8.9	14.6	17.1	»
30		22.50.57	130	7.7	10.6	13.5	18.6	27.7	41.5	drapery
31		51.19	135	7.8	11.4	14.0	18.6	29.2	44.5	»
32	18. 11. 1937	21.31.00	185	42.6	52.5	61.7	46.2	61.0	78.5	ray
33	30. 11. »	16 1.00	139	13.1	15.1	17.3	19.2	26.2	37.2	drapery
34		1.16	135	13.6	16.8	19.6	21.7	28.7	37.8	»
35		9.57	126	8.6	10.4	12.6	16.2	22.5	29.7	»
36	1. 12. »	16.19.41	157	20.6	26.7	33.0	29.0	44.3	63.6	»
37	19. 1. 1938	16.52.05	114	5.8	7.6	9.7	11.6	17.6	25.6	arc
38	5. 10. 1943	19.40.00	117	6.6	8.5	10.0	13.6	17.8	23.1	»
39	24. 11. »	20.42.00	135	11.2	13.8	16.6				faint arc
40		43.20	130	10.0	12.1	14.5				» »
41	1. 12. »	20.27.30	120	6.0	7.7	9.3	9.8	15.5	24.0	arc
42	23. 3. 1944	23.39.00	136	8.4	12.0	14.3				»
43	25. 3. »	21.25.00	152	17.6	22.4	26.0	24.9	33.3	43.2	drapery
44		34.15	162	21.8	32.6	49.0				ray-drap.
45		35.20	162	21.7	29.6	45.0	39.8	51.2	71.1	» »
46		36.00	153	19.4	25.3	32.0	31.9	45.8	65.0	» »
47		44.00	154	17.0	20.8	24.8	23.4	34.8	45.5	» »
48		44.50	134	10.2	15.4	20.1	13.1	26.2		drap.-band
49		47.00	124	6.4	10.0	12.6	13.3	20.4	30.0	arc
50		50.00	163	19.1	26.0	33.0	23.6	33.8	52.5	ray
51		52.30	140	11.3	15.4	21.3	15.9	26.4	41.0	drapery
52		53.00	133	11.0	13.6	15.9	12.8	19.0	30.4	»
53		54.00	152	12.9	16.4	20.8	17.8	26.6	39.8	»
54		55.00	151	12.6	16.3	24.3	17.6	25.0	36.0	»

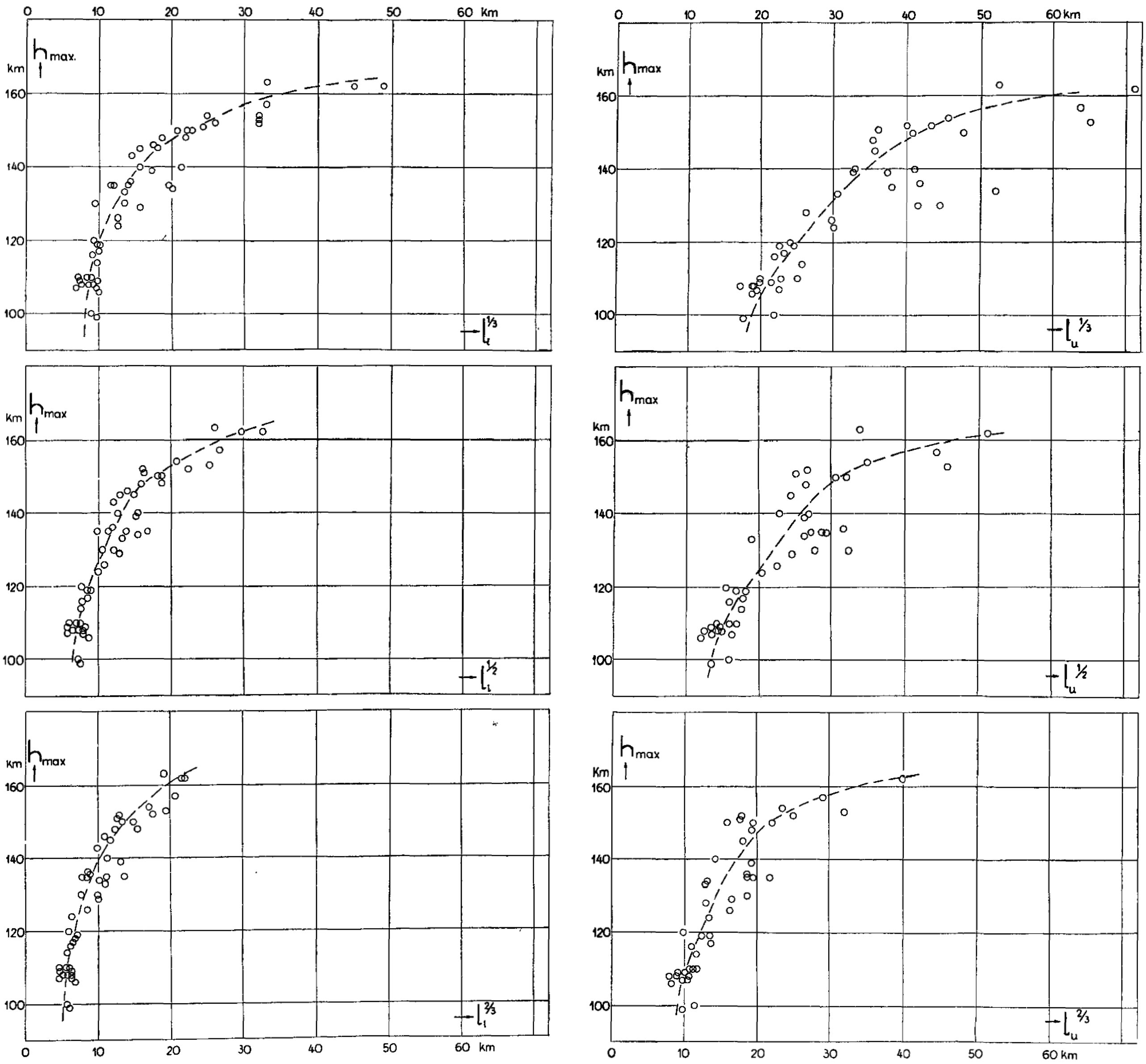

Fig. 6 *a* and *b*. Variation of $l_l^{2/3}$, $l_l^{1/2}$, $l_l^{1/3}$ and $l_u^{2/3}$, $l_u^{1/2}$, $l_u^{1/3}$ as functions of h_{max}

maximum h_{max}. In the region 100—160 km the value of H determined from the lower part of the luminosity curve is somewhat smaller than the value determined from the upper part. In this region the lower part of the luminosity curve decreases somewhat more rapidly than the ideal luminosity curve for the constant value of H, but this effect is small and we may say that for arcs and draperies in the lower part of the auroral region the character of the luminosity curve comes near to the ideal luminosity curve.

The two cases of rays, however, show a change in the values of H_l and H_u in the opposite direction, the values determined from the lower part of the luminosity being greater here than the values determined from the upper part. This corresponds to a slower decrease of the intensity at the lower part than is indicated by the ideal luminosity curve. In fact the high, faint rays often give the impression of being nearly symmetrical as regards the intensity of the lower and upper parts, see Nos. 11, 12, and 32 on Plates I and III. The high, sunlit rays reproduced in Størmer's papers[13] show the

[13] See for instance the reproduction in Terr. Mag. *44*, 11 (1939) of blue sunlit rays at a height of 250—500 km and in other papers by Størmer on high rays.

same feature. On the other hand the rays generally increase in length with increasing height, which should correspond to a general mean increase in the value of H in the atmosphere. In the case of high auroral rays the determination of the value of H_l will, therefore, generally be greater than H_u, a peculiarity which must be regarded as a *type*-effect for this special form.

Vegard has strongly advocated the point of view that the luminosity curve of the aurorae is strongly influenced by the spiral nature of the orbits of the electrically charged particles. If we assume that the value of ψ (*i. e.* the angle between orbit and the earth's magnetic field of force at the point where the particle enters the field) for the orbits of particles producing one single aurora or auroral ray comprises a certain series of values it is possible to construct several types of luminosity curves corresponding to different series of values of ψ[14]. By assuming a suitable series of ψ it is thus possible to construct a symmetrical luminosity curve or even a curve with a slighter decrease of intensity in the lower than in the upper part.

But there are other peculiarities of the intensity distribution of luminosity in the auroral rays. During very strong auroral displays faint auroral rays may occur which appear with almost uniform intensity from the upper limit of about 300 km down to the lower limit at 110 km.[15] There are also examples of rays and draperies with a short lower limit at about 105 km and a long, uniform and slight decrease to a upper limit of about 250 km.[16] Now the appearance of these rarer forms is associated with very strong magnetic storms. Radio echo experiments have now established, from the anomalous behaviour of the F_2-layer, that the atmosphere is strongly expanded during such conditions. The appearance of long auroral rays may, therefore, at least partly be explained by this effect. It must, however, be emphasized that there seems to be a difference in the character of the luminosity curves of the high rays and the arcs and draperies in the lower part of the auroral region. Further studies of rays, especially during *small* magnetic storms, would be of great interest.[17]

5. Comparison with Results of Ionospheric Studies.

In the previous sections the luminosity curve of the aurorae has been treated on the assumption that the orbits of the electrically charged particles can be regarded as rectilinear. For the high auroral rays this assumption, as previously mentioned, has led to certain discrepancies. For the lower aurorae the main luminosity curve must be regarded as similar to the theoretical luminosity curve for rectilinear propagation of the particles. If, however, the spiral nature of the orbits is taken into account, this will *diminish* the extension of the luminosity curve. The values of $H = kT/mg$ deduced experimentally from the luminosity curves are therefore to be regarded as the *minimum* values possible.

It is of considerable interest that the quantity $H = kT/mg$ can be determined from experimental studies of the ionosphere by a similar method. As previously mentioned, the construction of the luminosity curve and that of the curve giving the electron density within a simple layer are formally identical. By radio echo experiments we can determine the slope of the lower part of the electron density curve, from which the value of H can be estimated for the region concerned. *Appleton*[18]

[14] See *Vegard's* article, footnote 6, p. 608, for instance Fig. 11, type *c* and *d*. See also Størmer's paper, footnote 2, § 32, Fig. 26, where curves corresponding to different values of ψ are discussed.

[15] Such a case is described in *Harang:* Height Measurements of Selected Auroral Forms, Geof. Publ. *12*, No. 1, p. 8 (1937), see also Størmer's paper: Geof. Publ. *12*, No. 7, p. 12.

[16] A splendid example of such rays is reproduced in *Størmer's* paper: Über eine Nordlichtexpedition nach Trondheim in März 1933 Gerl. Beitr. z. Geophys. *41*, 382, pl. XII. In this case the upper half was sunlit.

[17] Of fundamental interest for the discussion of luminosity curves for H-determinations would be the appearance of special auroral forms with *short* vertical extensions at great heights. *Størmer* (Geof. Publ. *11*, No. 5, 1935, p. 5—11) has actually on three occasions measured very faint auroral *arcs* from Oslo with lower borders at the height of 193 km with the upper border at about 225 km. A vertical extension of only ca. 32 km at height of 200 km will give a value of H which is much smaller than the values deduced from our material at even lower heights. Now these arcs measured by Størmer were extremely faint and unfavourably situated for determinations of the upper limits. It is therefore possible that this material should not be regarded as reliable for H-determinations.

[18] *Appleton:* Regularities and Irregularities in the Ionosphere. I. Bakerian Lecture. Proc. Roy. Soc. *162*, 472 (1937) and Quart. Journ. Roy. Met. Soc. *65*, 327 (1939).

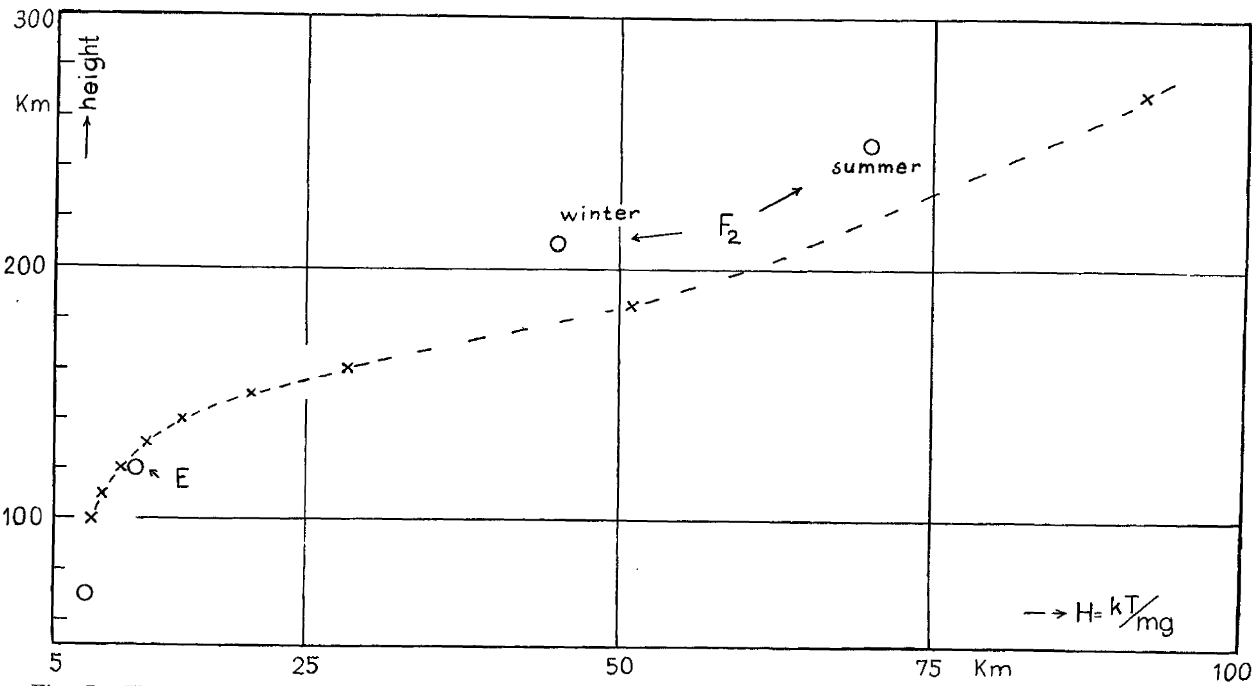

Fig. 7. Variation of $H = kT/mg$ with the height. x calculated from auroral luminosity curves. o calculated from ionospheric studies.

sums up the results of his determinations in South-East England:

$H =$ 11.4 km at 120 km (E-region),
$H =$ 40—50 km at 200 km upwards altering
to $H =$ 70 km at 250 km in summer (F_2-region).

From their studies of reflection of very long waves at the height of about 70 km *Budden, Ratcliffe* and *Wilkes* [19] conclude that at this height the value of H decreased to 7—8 km.

It is remarkable that the values calculated from the auroral luminosity curves and given in Table 5 coincide closely with the values of H deduced from ionospheric studies.

The inference from this would seem to be that, for arcs and draperies in the lower part of the auroral region, at 90—160 km, the orbits of the electrically charged particles may be regarded as nearly rectilinear, — assuming that the electrically charged particles are electrons.

Fig. 7 indicates the variations of $H = kT/mg$ with the height deduced from auroral and ionosperic observations.

From studies of the band-structure of the nitrogen bands 4278 Å and 3914 Å in the auroral spectrum, *Vegard* has determined the band temperature. The mean value of his determinations in the period 1923—1938 is 229° K [20]. If we assume this temperature to correspond to a mean level of 110 km, which should be the height of the intensity maximum of the strong auroral forms, the formula $H = kT/mg$ enables us to determine the mean molecular weight, using the value of $H = 8.8$ km determined from the mean auroral luminosity curve. We thus obtain for the level at 110 km the

mean molecular weight $m = 21.1$.

The mean molecular weight for complete mixing of O_2 and N_2 in the same proportions as at the ground is 28.95, and for complete dissociation the corresponding figure is 14.48. A mean molecular weight of 21.1 will therefore correspond to 54 % dissociation at the 110 km level. A partial dissociation of the atmosphere in the auroral region is also in accordanse with views now generally accepted for the constitution of the upper atmosphere.

In order to show the different alternatives of temperature variations with the heights, the T-values in Table 6, corresponding to three values of the mean molecular weights, $m = 21.1$, 28.95, and 14.48, have been calculated from the mean values of H determined from the luminosity curves.

[19] *Budden, Ratcliffe* and *Wilkes:* Further Investigations of very Long Waves Reflected from the Ionosphere. Proc. Roy. Soc. *171,* 188—214 (1939).

[20] Loc. cit., footnote 6, p. 646.

Table 6.

h	($m = 21.1$) T	($m=28.95$) T	($m = 14.48$) T
km	°	°	°
100	208	285	—
110	229	314	—
120	268	368	—
130	320	440	—
140	395	543	272
150	512	703	352
160	735	1010	505
185	(1325)	(1820)	(910)
270	(2390)	(3250)	(1625)

Assuming the absence of light gases in the auroral region, the temperature variation should, according to this table, lie between the values that correspond to values of m between 21.1 and 14.48. This temperature variation, which is determined exclusively from auroral evidences, is near the temperature variation proposed by *Martyn* and *Pulley*,[21] which was mainly based on the reflection of radio waves and collision frequency determinations in the ionosphere.

In the preceding discussions it is assumed that molecules and ions of the gases in the atmosphere are only exposed to the forces of gravity, and that the net volume charge of electricity per ccm is zero. *Vegard*[22] has advanced the theory that electric fields are present in the upper atmosphere, by which the distribution of the ionized matter is altered. The effect of the electric fields is, according to Vegard, to increase the density at greater heights above the values calculated from the usual barometric formula of height. The high temperatures at greater heights, which both ionospheric and auroral evidences imply, when they are treated along the lines given in the preceding sections, are thus avoided.

6. Change in Mean Heights of the Aurorae with Variation in χ.

Equation (6) shows that the height h' of the maximum luminosity is a function of the angle of incidence χ, which is the complement of the inclination I. From (6) we deduce the following equation:

$$h'_\chi - h'_o = H \text{ lognat sec } \chi, \qquad (11)$$

where h'_0 is the height of luminosity maximum corresponding to $\chi = 0$. The following numerical values are calculated from (11):

[21] Proc. Roy. Soc. *154*, 455 (1936).

[22] See for example, footnote 10, p. 647—651.

Table 7.

	I	χ	$h'_\chi - h'_o$
	90°	0°	0
Tromsø:	77	13	0.26 H
Oslo...	68	22	0.76 »
	60	30	1.44 »
	50	40	2.67 »
	40	50	4.02 «

The only two places for which the height frequency curves of the aurorae have been determined on the basis of more extensive material are over northern and southern Norway, corresponding roughly to the values of the inclination at Tromsø and Oslo. Between these two places the displacement of the maximum luminosity should be 0.5 H. Assuming H to be of the order of 10 km the displacement should be 5 km. *Størmer's* measurements from Oslo[23] indicate that the height of the lower border of aurorae over southern Norway are of the same order as those measured near the auroral zone. A displacement of only 5 km is, however, too small to be decided from the height frequency curves so far obtained. In lower latitudes there should be a considerable increase in the heights and vertical extensions of the auroral forms. Now the aurorae in lower latitudes only occur when associated with very great magnetic storms, during which such forms as rays and draperies predominate. Height determinations are still lacking, but judging from visual observations the aurorae appearing at low latitudes mainly appear as long streamers or draperies with great vertical extensions.*

[23] *Størmer:* Résultats des mésures photogrammétriques etc. Geofys. Publ. *4*, No. 7 (1926).

* Note added in proof: From a recent statistical survey of about 10 000 determinations of single points in the aurorae photographed over base-lines from Oslo Størmer has, however, shown that there is a small displacement in the height frequency curves for aurorae lying in different angular distances, Θ, from the earth's magnetic axis' point. This great material of height determinations was devided into two parts according to the position of the aurorae corresponding to $\Theta \geqq 30°$ or $\Theta \leqq 30°$. The value $\Theta = 30°$ roughly corresponds to Oslo. The statistics show that there is a displacement of about 2 km between the two height frequency curves, the aurorae with the greater angular distances from the earth's magnetic axis' point are lying at greater heights. (Preliminary communication in "Fra Fysikkens Verden", *7*, 180, 1945, Oslo.)

Table 8.

			G-photographs						V-photographs					
No.	Date	MET	$l_l^{2/3}$	$l_l^{1/2}$	$l_l^{1/3}$	$l_u^{2/3}$	$l_u^{1/2}$	$l_u^{1/3}$	$l_l^{2/3}$	$l_l^{1/2}$	$l_l^{1/3}$	$l_u^{2/3}$	$l_u^{1/2}$	$l_u^{1/3}$
			km	km	km	km	km	km	km	km	km	km	km	km
1	18. 11. 1935	17.40	6.55	8.42	—	9.42	26.33	32.40	7.41	9.34	11.60	10.75	30.08	40.02
2		42	7.54	9.56	12.08	11.02	16.53	21.78	7.98	10.30	12.75	11.00	18.25	27.25
3		51	8.68	11.60	14.23	8.90	12.45	17.60	10.45	12.45	14.70	13.80	19.60	25.40
4	21. 1. 1936	20.52	7.20	9.72	12.60	9.18	12.95	19.10	9.00	11.89	14.77	13.50	19.10	27.36
5	26. 1. «	17.05	8.32	10.10	12.84	11.20	15.56	21.20	9.00	11.48	13.70	12.42	17.60	23.38
6		9	6.16	7.82	9.51	10.58	15.93	21.70	6.16	8.35	10.45	9.77	16.10	23.30
7		46	5.07	6.48	7.90	9.87	14.25	19.75	6.91	8.45	10.15	12.00	20.30	28.50
8		22.03	4.55	5.45	6.63	7.53	10.40	17.25	5.46	6.89	10.90	8.58	12.75	18.45
9	16. 2. 1936	21.05	4.22	5.82	7.47	10.00	23.30	28.40	5.36	6.32	8.05	11.20	26.50	39.40
		Means:	6.48	8.33	10.41	9.47	16.30	22.13	7.53	9.50	11.97	11.45	20.03	28.12

7. Determinations of $H = kT/mg$ from Filter Photographs.

In principle the most complete solution of our luminosity curve studies would be a determination of the luminosity curve for each spectral line in the auroral form. A step in this direction has been made by means of filter photography. By using suitable filters the auroral spectrum was divided into two parts, one comprising only the green oxygen line 5577 Å, the other, the violet part, consisting mainly of the nitrogen bands 4708, 4278, and 3914 Å. Two identical cameras were furnished with these gelatine filters and simultaneous photographs were thus taken in green (*G*) and violet (*V*) of the auroral forms. The technique and reduction of the photographs has been described in a previous paper[8]

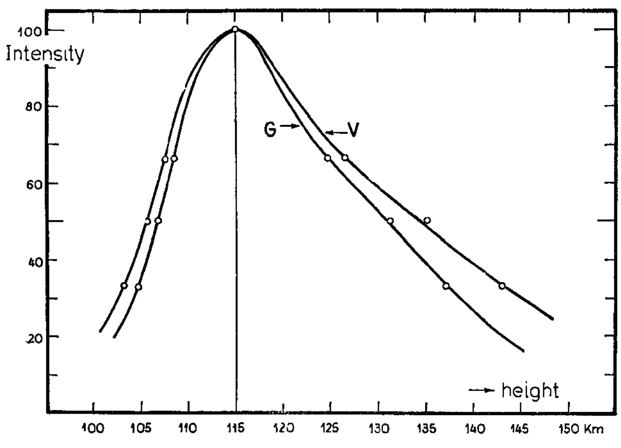

Fig. 8. Mean variation in green (5577 Å) and violet 4708, 4278, and 3914 Å) of a strong auroral arc.

and need not to be repeated here. The photographs used were taken during the winter 1935—36, and were of strong, diffuse arcs. Parallactic photographs were not taken, but as the mean heights of the strong arcs are well known, we have assumed a height of 115 km for the luminosity maximum.

Table 8 gives the distances to the points where the intensities have decreased to ⅔, ½, and ⅓ of the maximum intensity.

The mean variation in intensity in *G* and *V* of a strong auroral arc is illustrated in Fig. 8.

From the mean *l*-values in Table 8 the *H*-values are calculated in the same way as in section 6:

from *G*-photographs:

$$H_l = \frac{6.48}{0.786} = 8.26 \text{ km}$$

and

$$H_u = \frac{9.74}{1.058} = 9.36 \text{ »}$$

$$H_G = 8.81 \text{ km}$$

from *V*-photographs:

$$H_l = \frac{7.53}{0.786} = 9.58 \text{ km}$$

and

$$H_u = \frac{11.45}{1.058} = 10.32 \text{ »}$$

$$H_V = 9.95 \text{ km}$$

The mean value of the *G*- and *V*-values is 9.38 km at an assumed height of 115 km of the maximum intensity. This value fits in well with the mean values in Table 5 determined from ordinary auroral photographs.

In the formula $H = kT/mg$ we have to use the molecular weight of the oxygen and nitrogen molecule when calculating T from the H_G and H_V values, as the distribution of density is determined by the molecular weight according to the barometric height formula. The formula $H = kT/mg$ thus gives us:

$H_{N_2}/H_{O_2} = m_{O_2}/m_{N_2} = 32/28 = 1.143.$

From the luminosity curves observed we get:

$H_V/H_G = 9.95/8.81 = 1.13.$

Within the limit of error these two quantities coincide.

The increase of intensity of the violet nitrogen bands relatively to the green line with increasing height above the maximum intensity of arcs and bands was first shown by *Vegard* [24] and has since been extensively studied.

From the numerical data above we see that the effect of the increased intensity of the nitrogen bands both *above and below* the maximum intensity can be explained on the hypothesis that the nitrogen and oxygen molecules are separated with increasing height at a rate determined by the action of gravity.*

If this view is accepted it will have certain consequences for the atomic processes proposed for the exitation of the green auroral line.

As previously mentioned, it is now generally accepted that a certain fraction of the oxygen molecules is dissociated in the auroral region, a view supported by the discussion of the luminosity curves in Section 4. For the formation of free oxygen atoms different processes have been proposed by *Vegard* [25] and *Chapman.* Common to the processes proposed is the assumption of a state of equilibrium between the number of oxygen molecules and atoms at a certain height. The results of the discussion of the luminosity curves from the filter photographs indicate, however, that at the height interval where the arcs appear, the increase and separation of O_2 molecules relatively to N_2 molecules follows the barometric height formula. If, therefore, a portion of the oxygen molecules is dissociated it follows from the discussion above that this percentage of dissociation must be fairly *constant* within the height interval where the arcs appear. We are further forced to assume that the percentage of dissociated O_2 molecules is so low that the mean molecular weight of O and O_2 is nearly equal to the molecular weight of O_2.

This view does not agree with the far higher rate of dissociation which was deduced from the luminosity curves in Section 4, where the band temperature was used in calculating the mean molecular weight in the formula for H. The weak point in this deduction is, however, that the spectroscopally determined band-temperature is assumed to be equal to the gas kinetic temperature used in the barometric height formula. The final decision regarding this uncertainty in the assumption of the rate of dissociation will be left open until further theoretical and experimental evidence is available.

If we take the assumption of a constant and low percentage of dissociation of the O_2 molecules to be valid for the whole auroral region up to a height of 500—800 km, we get the following picture of the intensity variations between the green and violet parts of the auroral spectrum:

a) In the same auroral form we have a decrease *above and below* the maximum intensity of the relative intensity of 5577 compared with the nitrogen bands of the type shown by the filter photographs of the arcs. This is explained by the properties of the luminosity curve of a radiation penetrating into an atmosphere consisting of O_2 and N_2. *b*) There is a *general* decrease of the intensity of the auroral forms in 5577 Å with height, as compared with the luminosity in the violet which is due to a decrease in concentration of O_2 with the height. This effect seems to be the one observed in the high auroral rays investigated by *Størmer.* [26]

According to the view set forth here, the relative increase of the intensity of the nitrogen bands in the upper part of an arc does not permit as to extrapolate this increase to a general increase of

* In the case above we have compared the intensity variation of the nitrogen bands with the *green* auroral line. If, however, the intensity of the nitrogen bands is compared with other oxygen lines, the red lines 6300, 6363 Å, we would get a variation with height in the opposite direction. The red lines 6300, 6363 Å show an increse with height relatively to the green line and even to the nitrogen bands, as shown by Vegard.

[24] *Vegard:* Handb. d. Exp.phys. *25,* 453 (1928), see also Zs. f. Geophys. *6,* 42 (1930).

[25] *Vegard:* Erg. exakt. Naturwiss. *17,* p. 254—258 (1938). *Chapman:* On the Production of Auroral and Night-Sky Light, Phil. Mag. *23,* 657—665 (1937).

[26] *Størmer.* Sonnenbelichtete Nordlichtstrahlen, Zs. f. Geophys. *5,* 177 (1929).

the nitrogen bands in aurorae at great heights. What we have to measure is the relative intensities of green and violet at the *maximum intensity* of aurorae situated at different heights above the earth's surface.

In future researches by filter photography it will be of interest to investigate the change in the ratio between the maximum intensities in G- and V-photographs of aurorae at different heights. It would be especially interesting to secure filter photographs of the high, auroral rays, in order to determine the intensity distribution in G and V. This will be difficult on account of the low general intensity in G, but with the increasing speed of modern orthocromatic plates it should be possible in some cases.

In the discussion and interpretation of the luminosity curve, a schematic picture of a bundle of cathode rays of constant cross-section penetrating the atmosphere has been used. During its passage into the atmosphere the bundle will be liable to scattering, which may modify the results. Further, there is a certain decrease of velocity of the corpuscles along the ray, caused by the successive collisions. This latter effect may have a special influence on the curve of exitation for the different spectral lines or bands.[27]

For cathode rays of great velocities, however, which are assumed to be the primary cause of the aurorae, this specific influence on the curve of exitation with decrease of velocity is small.

Density and Pressure of the Amosphere in the Auroral Region.

These quantities can be calculated if the variation of $H = kT/mg$ with the height h is known. In the preceding sections the variation of H has been derived from the luminosity curve of the aurorae, and if the assumptions made for this deduction are justified, the pressures and densities can easily be calculated. For the numerical calculations the atmosphere has been divided into a number of sections, each with a constant value of H according to Fig. 9. The values of H are given in Table 9.

[27] See for instance the article: *Hanle,* Die Lichtausbeute bei Stossanregung. Ergebn. d. exakt. Naturwiss. *10,* 285 (1931).

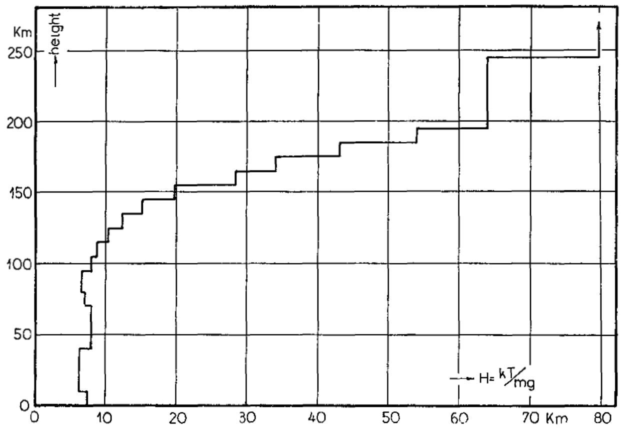

Fig. 9. Variation in steps of $H = kT/mg$ with height.

Table 9.

Interval of height	$H = kT/mg$	Interval of height	$H = kT/mg$
km	km	km	km
0— 10	7.5	125—135	12.3
10— 40	6.4	135—145	15.2
40— 70	8.0	145—155	19.7
70— 80	7.0	155—165	28.3
80— 95	6.5	165—175	34.0
95—105	8.0	175—185	43.0
105—115	8.8	185—195	54.0
115—125	10.3	195—245	64.0
		245— ∞	80.0

The results of the numerical calculations of the density ϱ and the pressure p are given in Table 10.

Table 10.

h	ϱ	p	h	ϱ	p
km	gr/cm³	gr/cm²	km	gr/cm³	gr/cm²
70	$7.33 \cdot 10^{-8}$	$5.09 \cdot 10^{-2}$	195	$2.83 \cdot 10^{-12}$	$2.03 \cdot 10^{-5}$
80	$1.75 \cdot 10^{-8}$	$1.18 \cdot 10^{-2}$	205	$2.42 \cdot 10^{-12}$	$1.77 \cdot 10^{-5}$
87	$5.95 \cdot 10^{-9}$	$5.24 \cdot 10^{-3}$	215	$2.07 \cdot 10^{-12}$	$1.54 \cdot 10^{-5}$
95	$1.72 \cdot 10^{-9}$	$1.49 \cdot 10^{-3}$	225	$1.77 \cdot 10^{-12}$	$1.34 \cdot 10^{-5}$
105	$4.88 \cdot 10^{-10}$	$5.02 \cdot 10^{-4}$	235	$1.52 \cdot 10^{-12}$	$1.18 \cdot 10^{-5}$
115	$1.56 \cdot 10^{-10}$	$2.09 \cdot 10^{-4}$	245	$1.30 \cdot 10^{-12}$	$1.04 \cdot 10^{-5}$
125	$5.92 \cdot 10^{-11}$	$1.09 \cdot 10^{-4}$	270	$9.50 \cdot 10^{-13}$	$7.60 \cdot 10^{-6}$
135	$2.63 \cdot 10^{-11}$	$6.91 \cdot 10^{-5}$	300	$6.52 \cdot 10^{-13}$	$5.22 \cdot 10^{-6}$
145	$1.36 \cdot 10^{-11}$	$4.98 \cdot 10^{-5}$	350	$3.49 \cdot 10^{-13}$	$2.78 \cdot 10^{-6}$
155	$8.20 \cdot 10^{-12}$	$3.91 \cdot 10^{-5}$	400	$1.87 \cdot 10^{-13}$	$1.50 \cdot 10^{-6}$
165	$5.76 \cdot 10^{-12}$	$3.22 \cdot 10^{-5}$	500	$5.34 \cdot 10^{-14}$	$4.27 \cdot 10^{-7}$
175	$4.30 \cdot 10^{-12}$	$2.72 \cdot 10^{-5}$	600	$1.53 \cdot 10^{-14}$	$1.22 \cdot 10^{-7}$
185	$3.41 \cdot 10^{-12}$	$2.33 \cdot 10^{-5}$	700	$4.36 \cdot 10^{-15}$	$3.49 \cdot 10^{-8}$
			800	$1.25 \cdot 10^{-15}$	$1.00 \cdot 10^{-8}$

9. Estimates of Velocities of the Cathode Rays Producing the Aurorae.

When the variation of pressure wtih height is known the absorption and luminosity curves for cathode rays of different velocities are easily calculated by using the formulas previously found. In what follows the absorption and luminosity curves of cathode rays with velocities in the series 0.02 c —0.9 c ($c =$ velocity of light) have been calculated. The coefficients of absorption (μ in $cm^{-1}/_{g/cm^3}$) used are given in Table 11.[28]

Table 11.

v/c	μ	v/c	μ
0.02	$1.3 \cdot 10^7$	0.5	$2.2 \cdot 10^2$
0.06	$2.5 \cdot 10^5$	0 6	83
0.1	$8.0 \cdot 10^5$	0.7	29
0.2	$3.6 \cdot 10^4$	0.8	13
0.3	$2.9 \cdot 10^2$	0.9	6
0.4	$7.4 \cdot 10^2$		

In Fig. 10 the curves of absorption and luminosity are demonstrated for the whole range of cathode rays.

In a previous paper[29] the mean heights of the aurorae in the form of arcs, bands and draperies have been discussed for various classes of intensities. It was shown that there was a systematic decrease of the height of the lower border with the increasing intensity of the auroral form. From the absorption and luminosity curves given above, it is now possible to estimate the mean variation in velocities of the cathode rays producing arcs and bands of varying intensities. Assuming 90 % absorption of the cathode rays at the lower border of the arcs and bands, the estimates of velocities are given in Table 12.

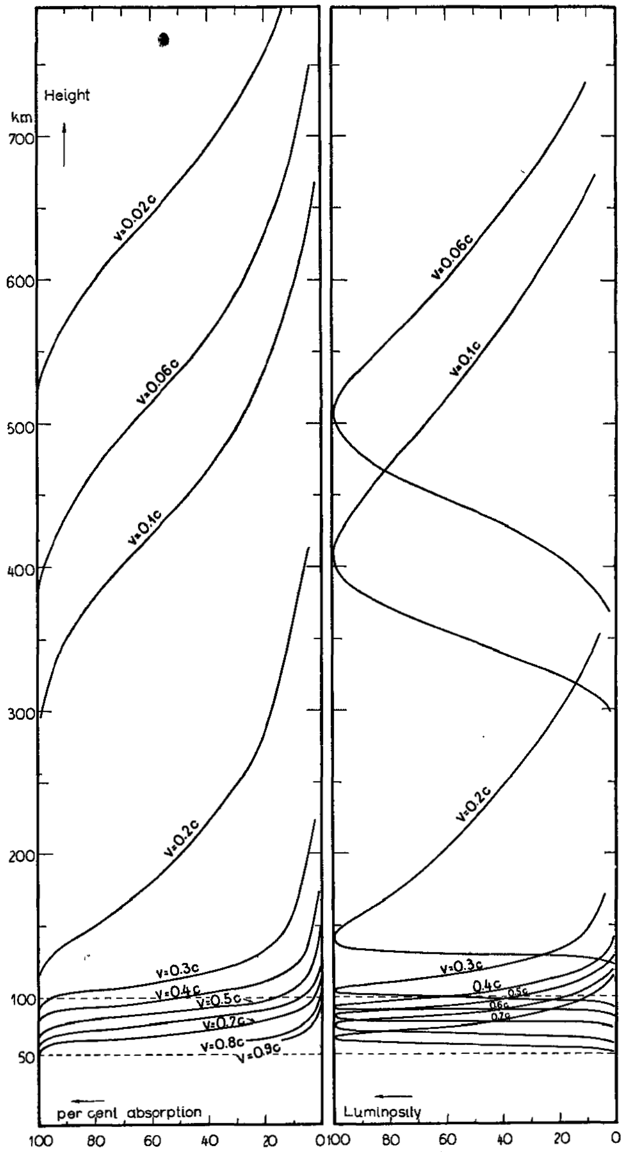

Fig. 10. Curves of absorption of cathode rays and curves of luminosity produced by the absorption, computed for cathode rays in the velocity series 0.02 c—0.9 c.

Table 12.

Mean height of lower border of arcs and bands of different intensities.	Velocities of cathode rays estimated.	Stiffness $H\varrho = mv/e$
Intensity low (2): 114.3 km	0.26 c	442
» medium (3): 108.0 »	0.28 »	476
» strong (4): 99.3 »	0.315 »	595
» very strong (5): 94.7 »	0.36 »	612
Arc with very strong red lower border measured in 1932[30]: 65—70 »	0.7 »	1190

[28] *Wien-Harms:* Handb. d. Exp.phys. *25*, Lenard-Becker: Kathodenstrahlen, p. 178 (1927).

[29] *Harang:* A Study of Auroral Arcs and Draperies. Geof. Publ. *13*, No. 14 (1944).

[30] *Harang* und *Bauer:* Über einen Nordlichtbogen in weniger als 80 km Höhe über die Erde. Gerl. Beitr. Geophys. *37*, 109 (1932).

10. The Height of the Auroral Luminosity and the Height of the Abnormal E-layer Occurring during Auroral Displays and Earthmagnetic Storms.

As previously explained there is a complete formal analogy between the construction of the auroral luminosity curve (L) and the electron density curve (N) in an ionized layer if we assume that both are produced by a "monochromatic" radiation penetrating the atmosphere rectilinearly.

The formation of the strong abnormal E-layer during a single auroral display must be due to the *same* bundle of radiation which produces the auroral luminosity. It is thus evident that during aurorae the luminosity curve (L) and the electron density curve (N) must both have the *same form* and lie in the *same height interval.*

During 1942 the appearance of the abnormal E-layer on a frequency of 3.65 Mgc/sec was recorded for several months. A fairly low "kipp"-velocity on the oscillograph corresponding to 20 mm/100 km was used, which made it possible to measure the height of the E-reflections with good accuracy. Fig. 11 shows the mean diurnal variation of the height of the abnormal E-reflections during one month.

The height of the reflecting lower boundary lies in the height interval 110—120 km. This corresponds to an height which lies only some km higher than the lower border of the aurorae. The lowest E-reflection measured is 94 km. Reflections from heights of 80—90 km, which correspond to the border of the very strong aurorae, have not been recorded. Now the echoes are always absorbed during very strong auroral displays, when the very strong aurorae of the lowest heights occur. We are thus unable to record the lowest possible values of the abnormal E-reflections. Accordingly we should expect that the mean reflection heights of the abnormal E-reflections would lie somewhat higher than the mean lower border of the aurorae, which is also in accordance with the echo records mentioned above.

In this discussion of the position of the abnormal E-reflections we have not taken into account the effect of recombination. We may assume that the recombination is more effective in the lower than in the upper part of the abnormal E-layer, which will slightly displace the curve of ionisation towards greater heights. We may take it, however, that the effect in this case is negligible.

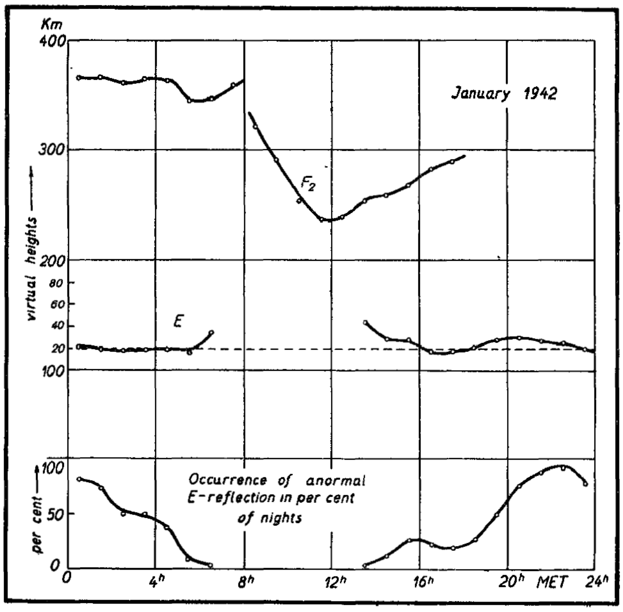

Fig. 11. Mean variation of the abnormal E-layer during one month recorded on a fixed frequency of 3.65 Mgc/sec.

Summing up the results we may say that the mean reflection heights of the abnormal E-reflections coincide with the mean heights of the lower boundary of the arcs and bands of *low* and *medium intensity* (114.3 and 108.0 km).[31]

The *region of absorption* of the radio waves during strong disturbances is thus restricted to the height interval where the lower borders of the *very strong aurorae* appear, *i. e.* to the interval of *80—90* km in height.

The layer of absorption has previously often been associated with a special layer, the hypothetical D-layer at an assumed height of 60—70 km. According to the argument above, however, it seems more reasonable to associate the layer of absorption with the lower part of the auroral region.

There is one *faint* form of aurorae, however, during the occurrence of which we usually observe complete absorption of the radio echo over the whole frequency band, it is during the pulsating surfaces or the "auroral clouds". Parallactic measurements show that this special form, which usually only appears after strong auroral displays at midnight or early in the morning, lies in the height interval of 80—95 km. The effect of absorption is thus

[31] See, footnote 29, p. 6.

to be expected, according to the view expressed above, during the occurrence of this faint form of aurora.

11. Summary.

The theoretical curve of luminosity produced by a bundle of cathode rays penetrating an atmosphere rectilinearly has been discussed.

The luminosity curve of aurorae has been determined by photographic photometric methods. The luminosity curves observed have been compared with the theoretical luminosity curve produced by cathode rays. The mean value of $H = kT/mg$ has been determined as a function of the height of the maximum luminosity. The values of H determined from studies of aurorae are in agreement with the values determined independently from ionospheric studies.

The values of H have been determined for the luminosity in green (G) and violet (V) independently from filter photographs.

Using the experimentally determined values of H the density and pressure in the auroral region have been computed for various heights. The curves of absorption and the luminosity curves for bundles of cathode rays in the range of velocities 0.02 c—0.9 c penetrating the model-atmosphere rectilinearly have been computed.

The height of the abnormal E-reflections observed during auroral displays, and the position of the absorbing layer, have been discussed.

The author wishes to express his sincere thanks to Mr. Steinar Jenssen for his assistance in the parallactic photography and to meteorologist K. Langlo for his valuable assistance in the radio echo observations.

Contents.

Printed, February 13, 1946.

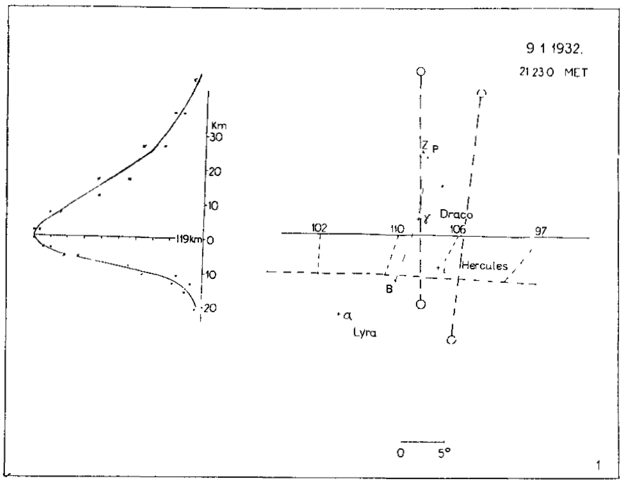
9 1 1932.
21 23 0 MET
Km
119 km
Draco
Hercules
Lyra
0 5°
1

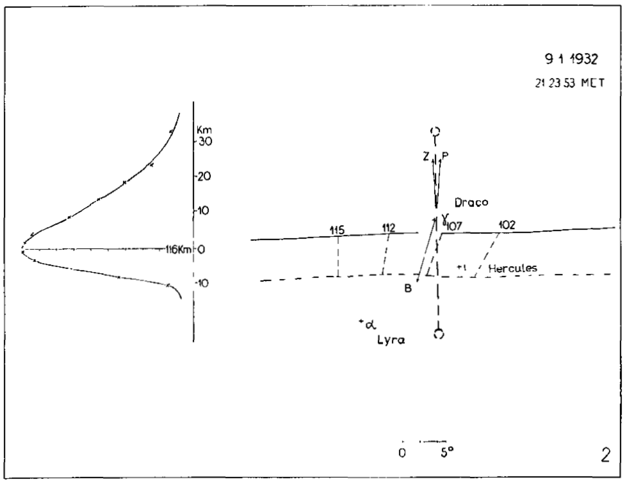
9 1 1932
21 23 53 MET
Km
116 Km
Draco
Hercules
Lyra
0 5°
2

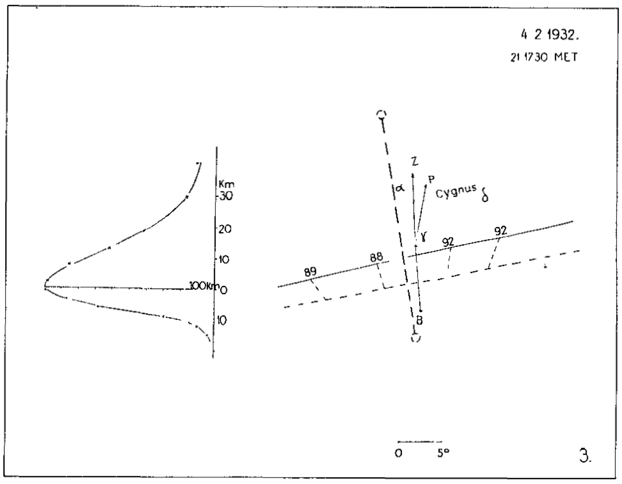
4 2 1932.
21 17 30 MET
Km
100 Km
Cygnus
0 5°
3.

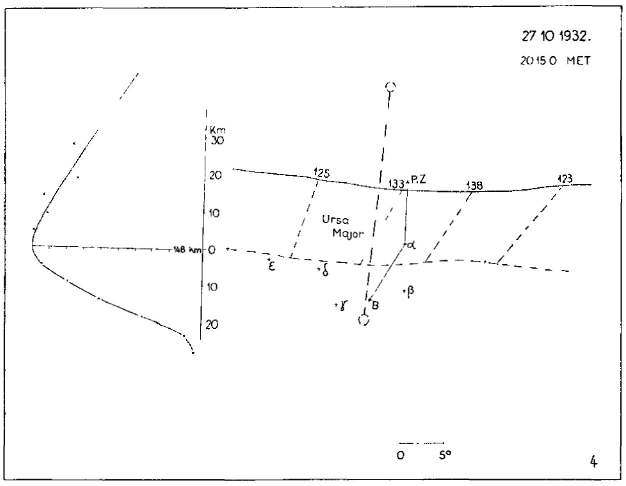
27 10 1932.
20 15 0 MET
Km
148 km
Ursa Major
0 5°
4

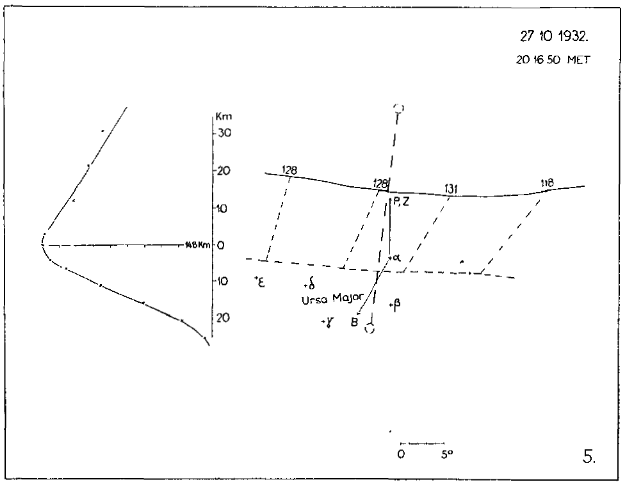
27 10 1932.
20 16 50 MET
Km
148 Km
Ursa Major
0 5°
5.

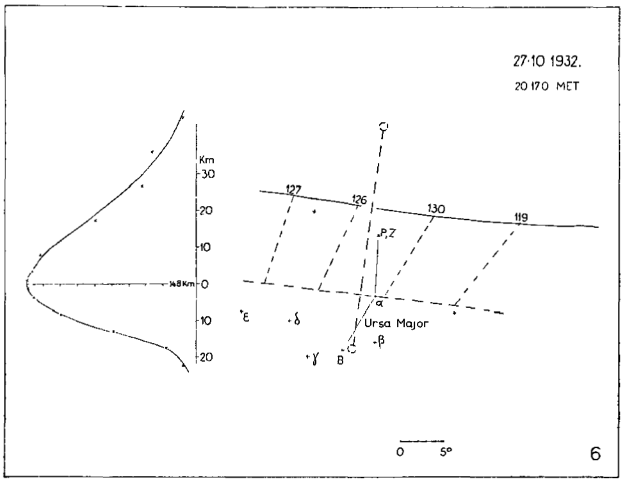
27·10 1932.
20 17 0 MET
Km
148 Km
Ursa Major
0 5°
6

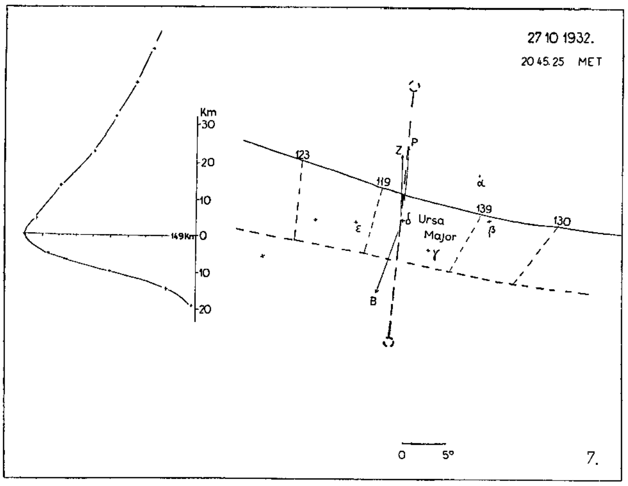
27 10 1932.
20 45 25 MET
Km
Ursa
Major
0 5°
7.

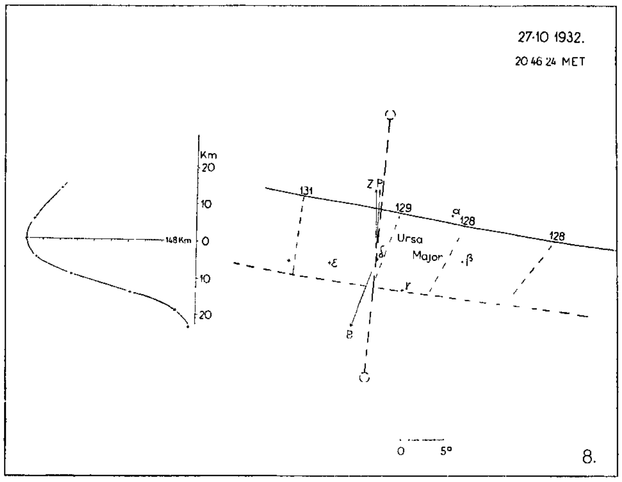
27·10 1932.
20 46 24 MET
Km
Ursa
Major
0 5°
8.

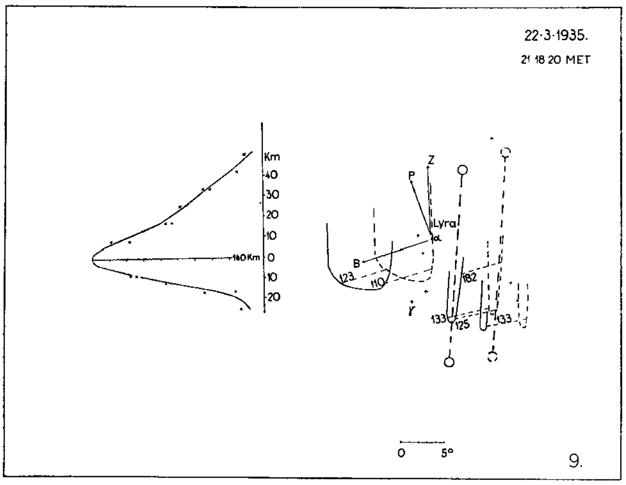
22·3·1935.
21 18 20 MET
Km
Lyra
0 5°
9.

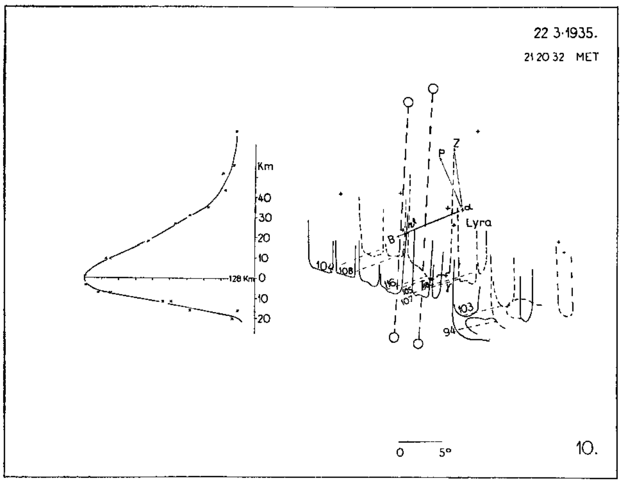
22 3·1935.
21 20 32 MET
Km
Lyra
0 5°
10.

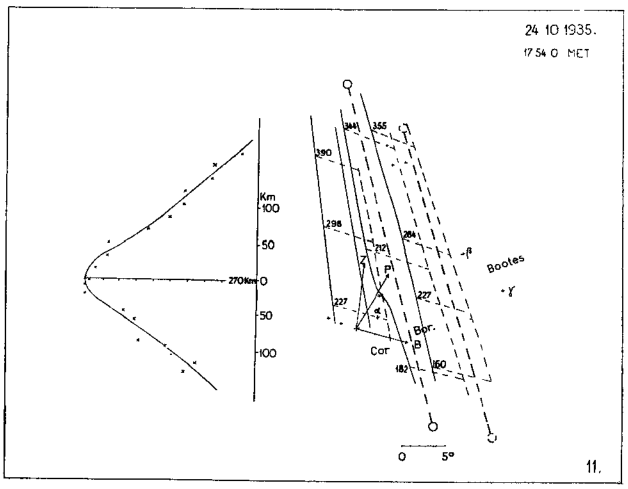
24 10 1935.
17 54 0 MET
Km
Bootes
Cor
Bor.
0 5°
11.

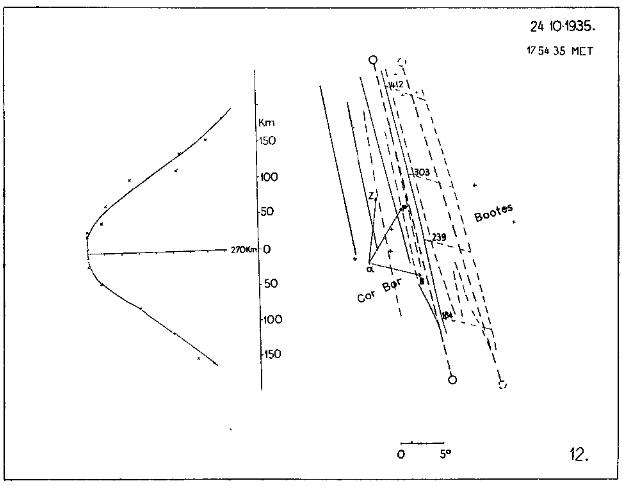
24 10·1935.
17 54 35 MET
Km
Bootes
Cor Bor
0 5°
12.

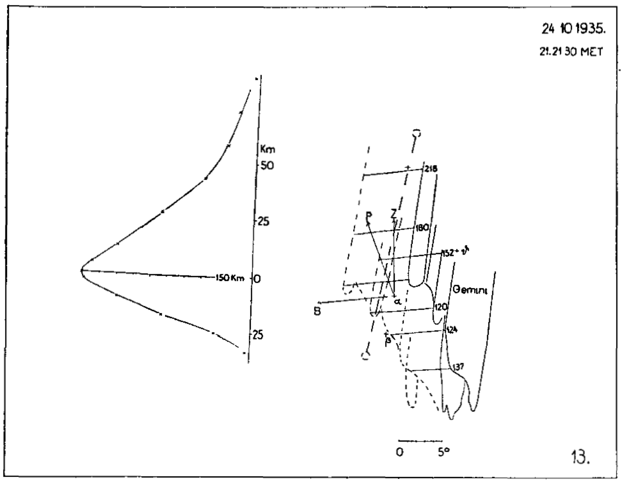
24 10 1935.
21.21 30 MET
Km
50
25
150 Km
0
25
P
Z
218
180
152
Gemini
B
α
β
120
124
137
0 5°
13.

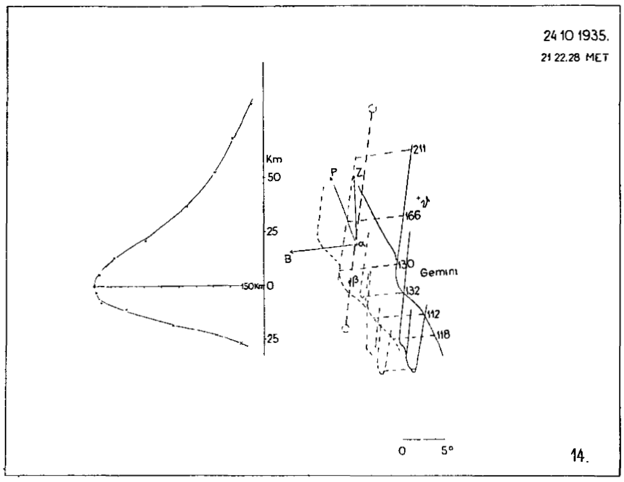
24 10 1935.
21 22.28 MET
Km
50
25
150Km
0
25
P
Z
211
166
130
Gemini
B
α
β
132
112
118
0 5°
14.

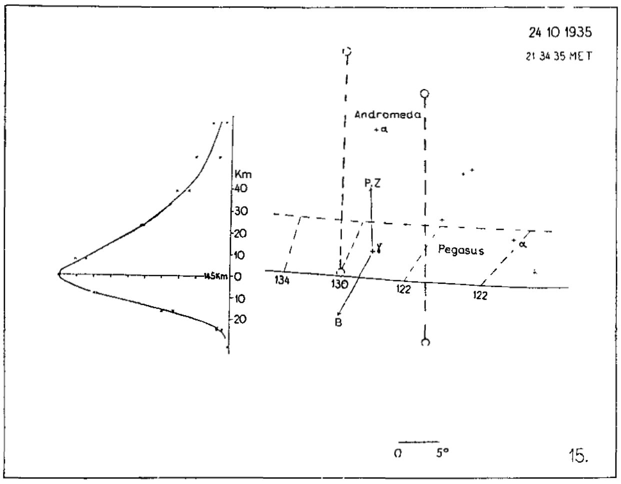
24 10 1935
21 34 35 MET
Andromeda
α
P,Z
Km
40
30
20
10
145Km
0
10
20
Pegasus
134
130
122
122
B
0 5°
15.

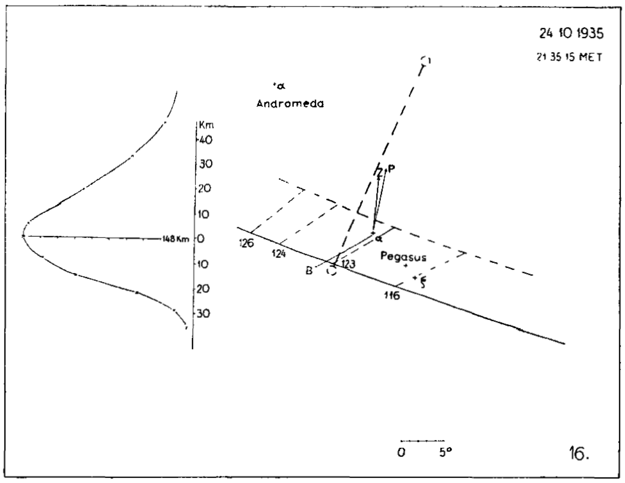
24 10 1935
21 35 15 MET
α
Andromeda
Km
40
30
20
10
148 Km
0
10
20
30
P
α
126
124
123
Pegasus
B
116
0 5°
16.

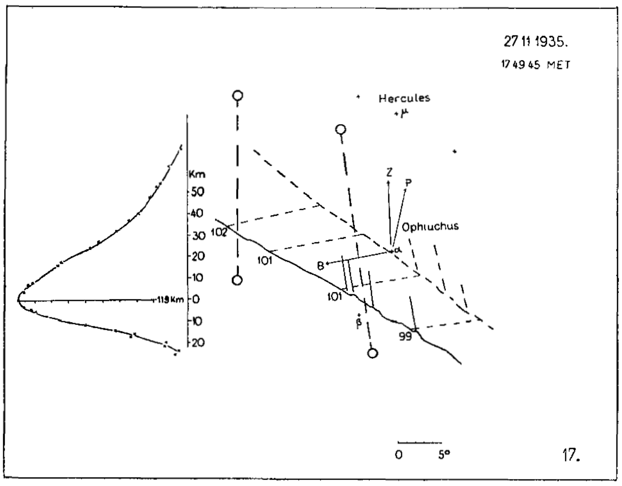
27 11 1935.
17 49 45 MET
Hercules
μ
Km
50
40
30
20
10
118 Km
0
10
20
Z
P
Ophiuchus
102
101
B
α
101
β
99
0 5°
17.

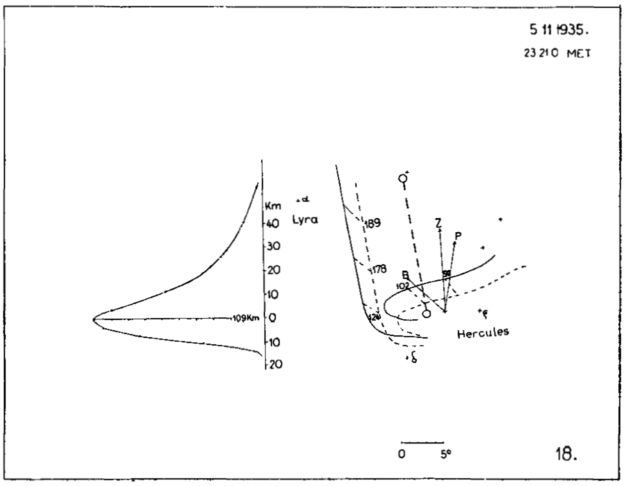
5 11 1935.
23 21 0 MET
Km
40
30
20
10
109Km
0
10
20
α
Lyra
189
178
Z
P
B
Hercules
0 5°
18.

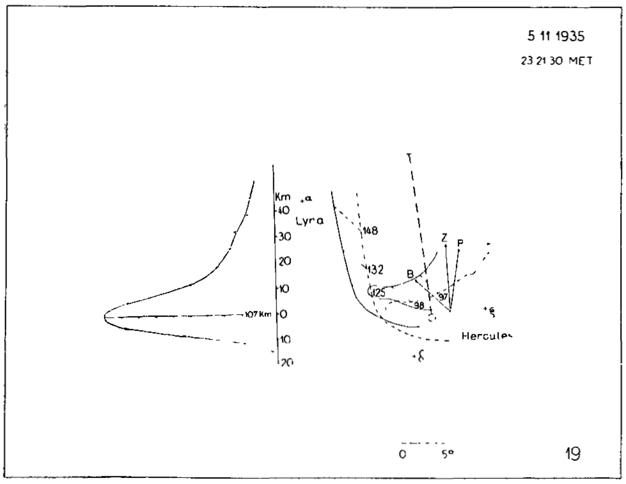

19

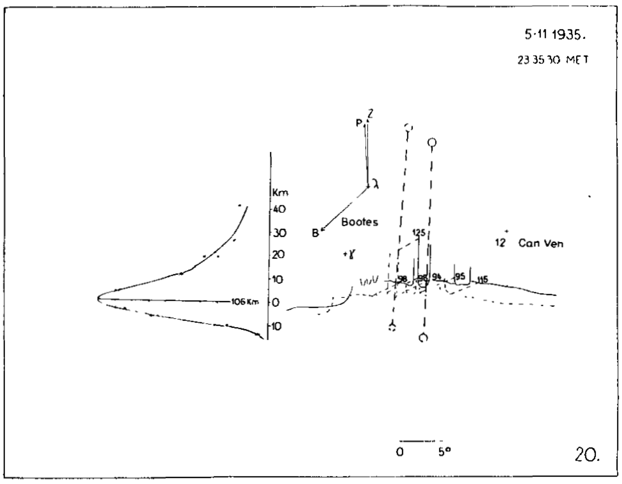

20.

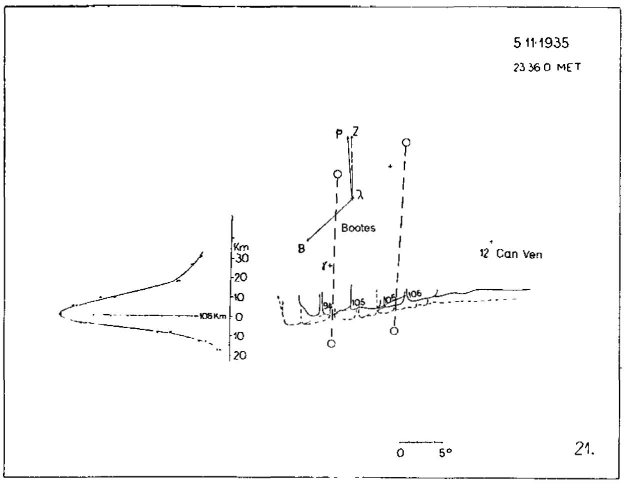

21.

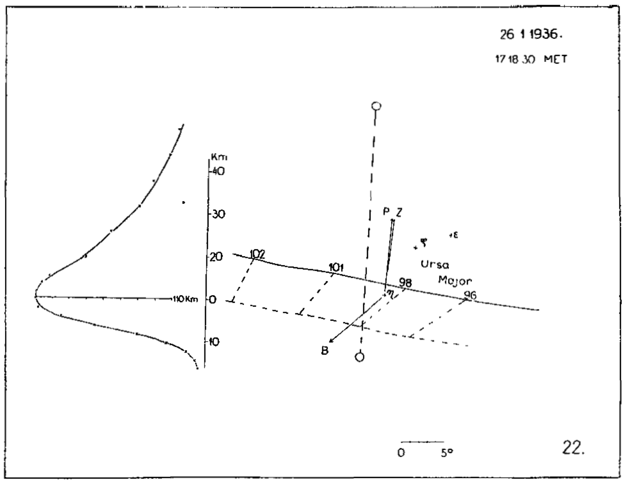

22.

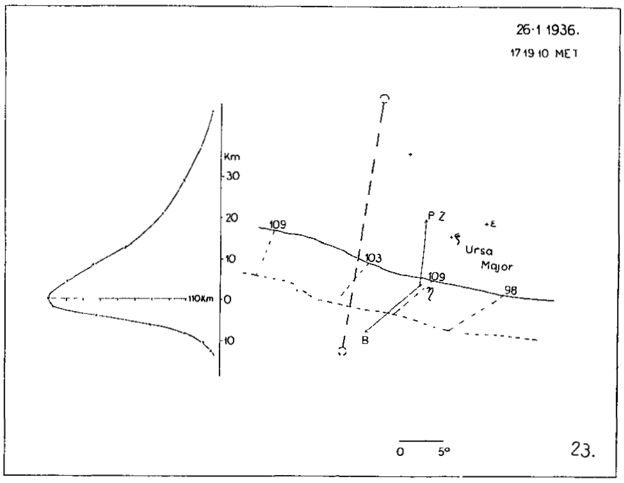

23.

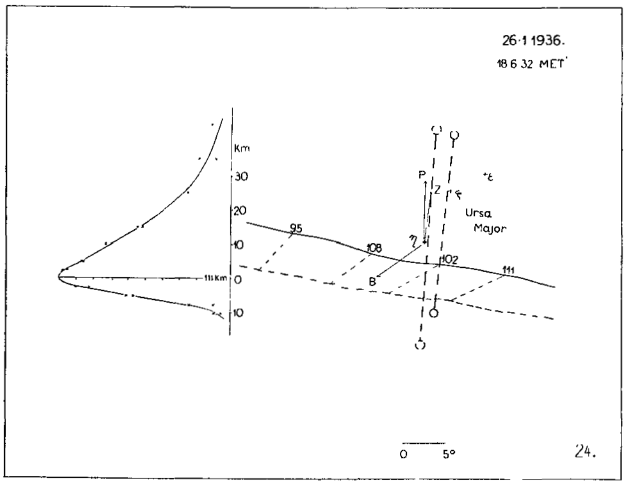

24.

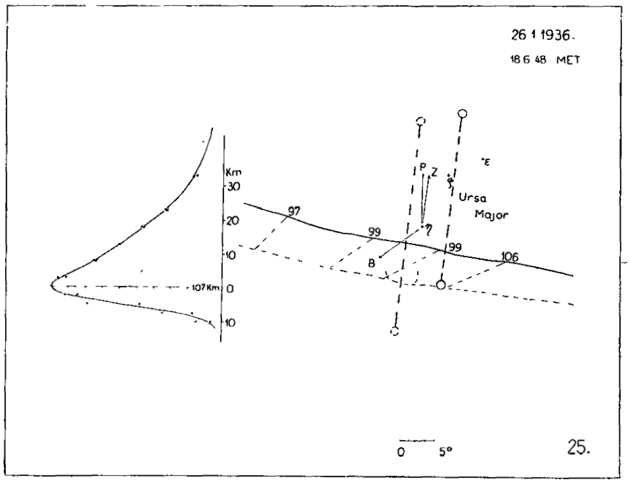

25.

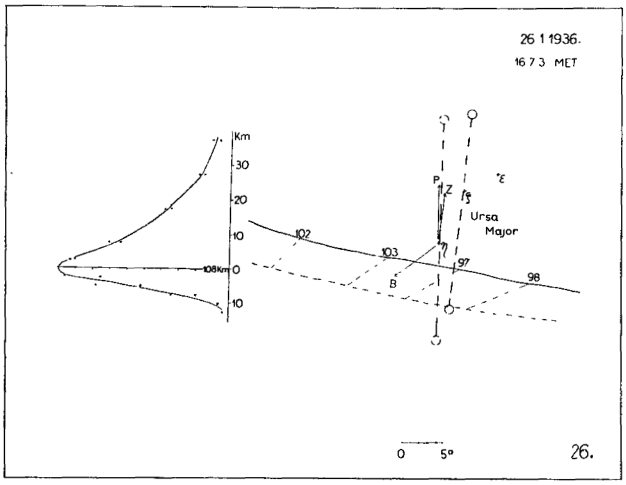

26.

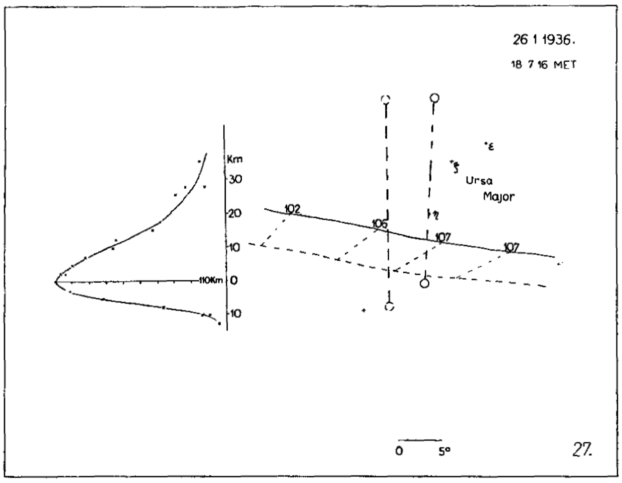

27.

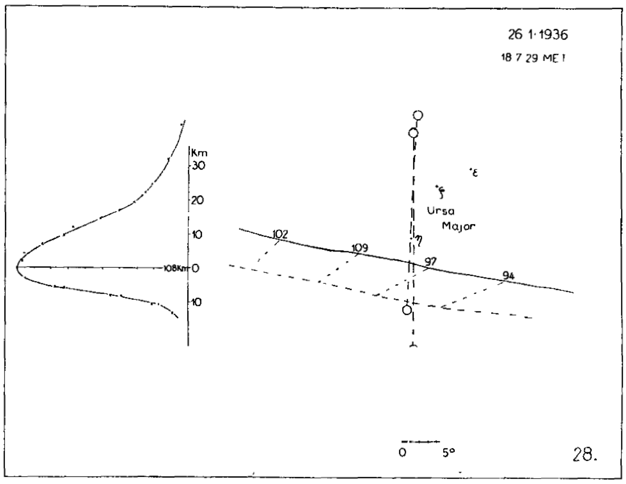

28.

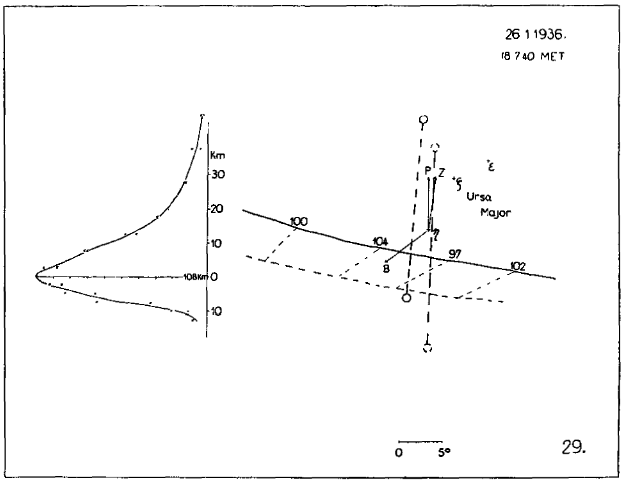

29.

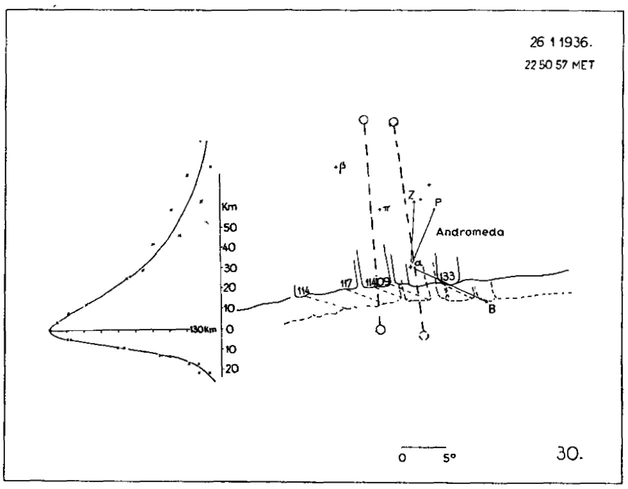

30.

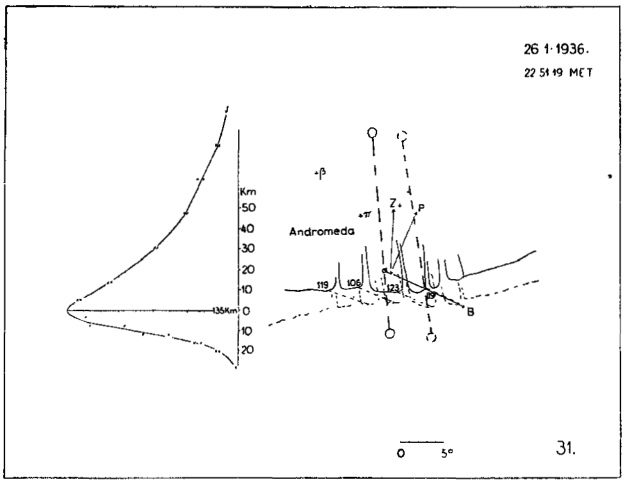

31.

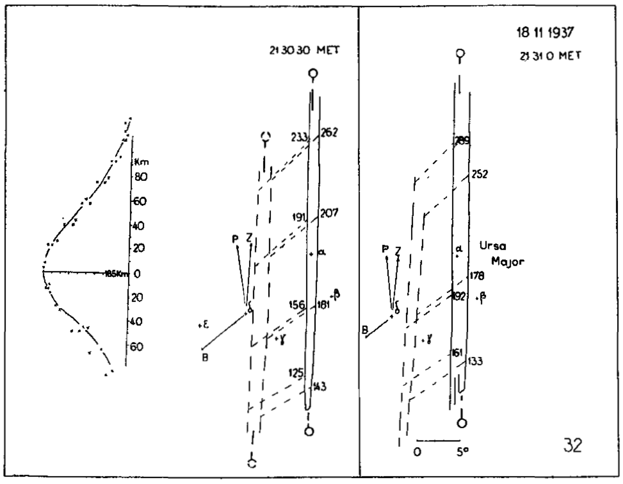

32

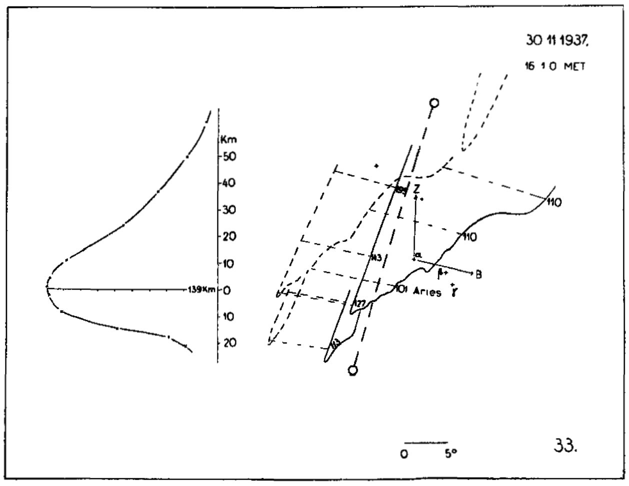

33.

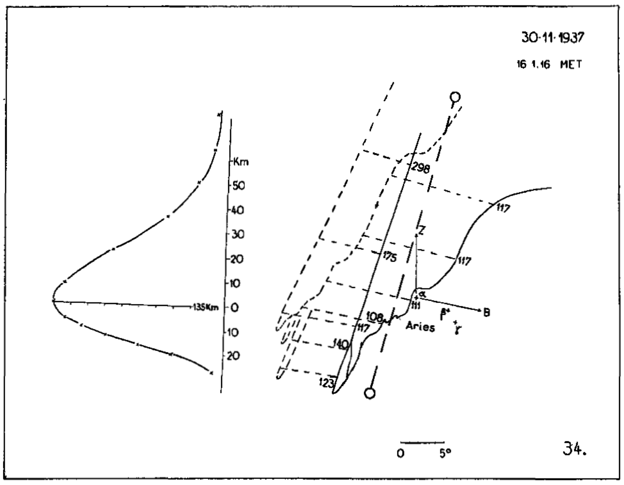

34.

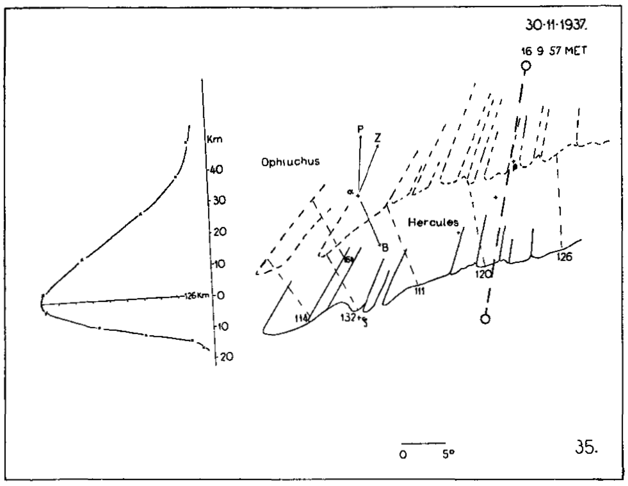

35.

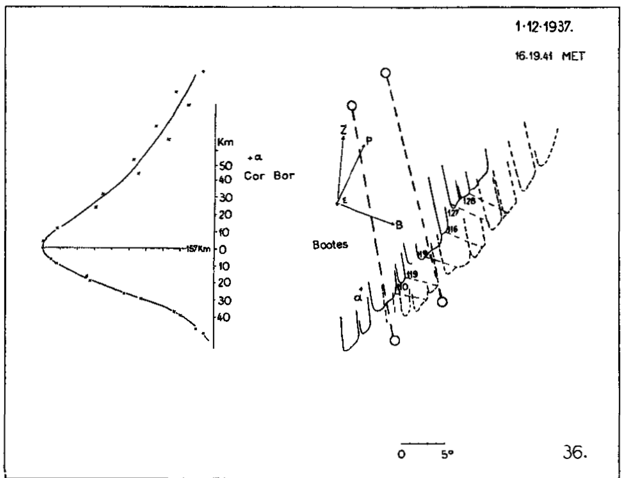

36.

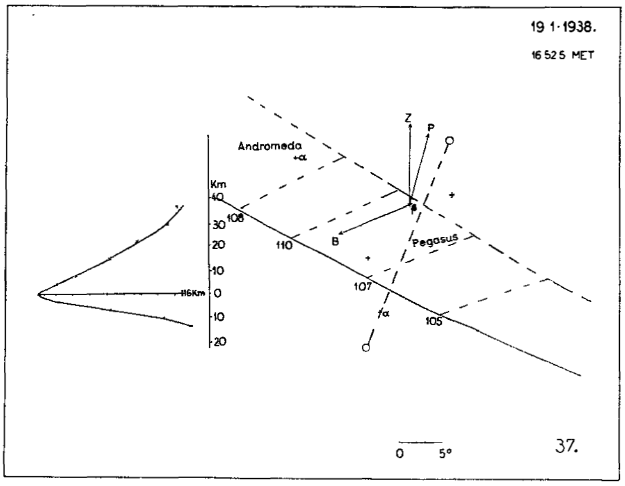
19 1·1938.
16 52.5 MET
Andromeda
Km
40
30
20
10
0
10
20
116Km
108
110
B
Z
P
Pegasus
107
105
0 5°
37.

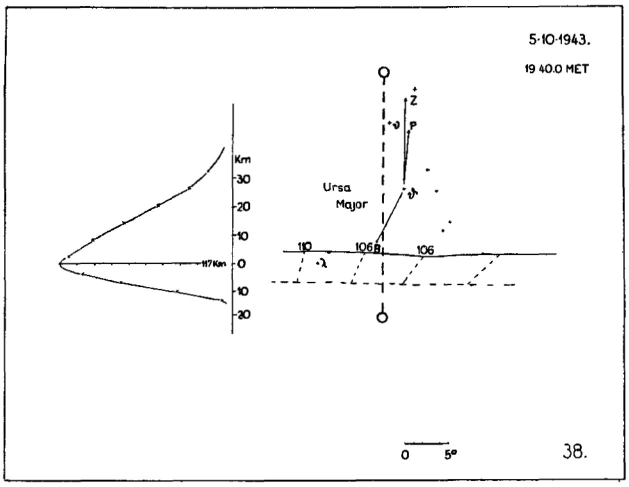
5·10·1943.
19 40.0 MET
Km
30
20
10
0
10
20
117Km
Ursa
Major
Z
P
110
106
106
0 5°
38.

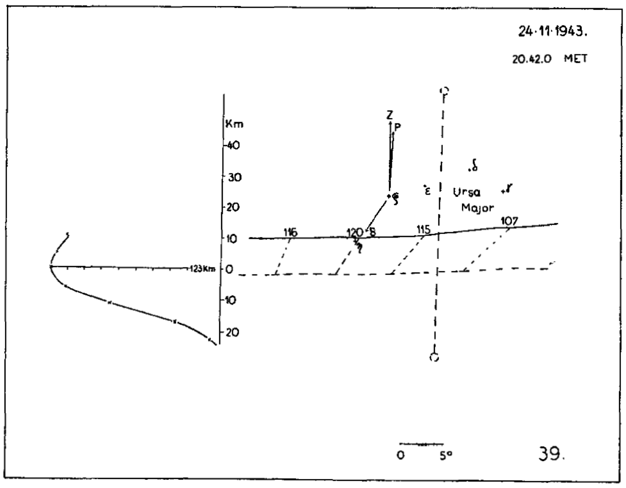
24·11·1943.
20.42.0 MET
Km
40
30
20
10
0
10
20
123Km
Z
P
Ursa
Major
116
120
B
115
107
0 5°
39.

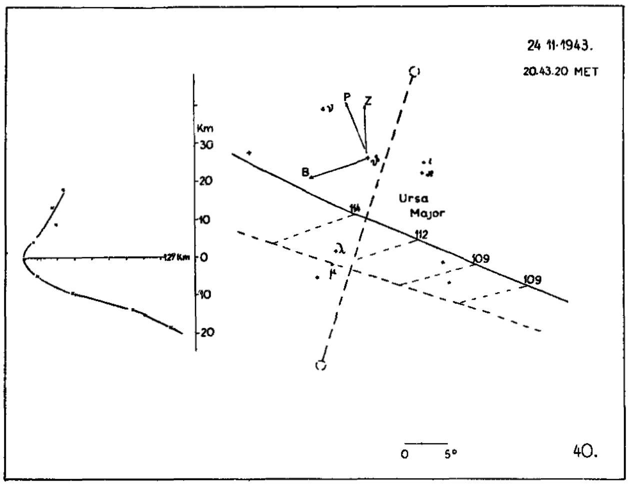
24 11·1943.
20.43.20 MET
Km
30
20
10
0
10
20
127Km
P
Z
B
Ursa
Major
114
112
109
109
0 5°
40.

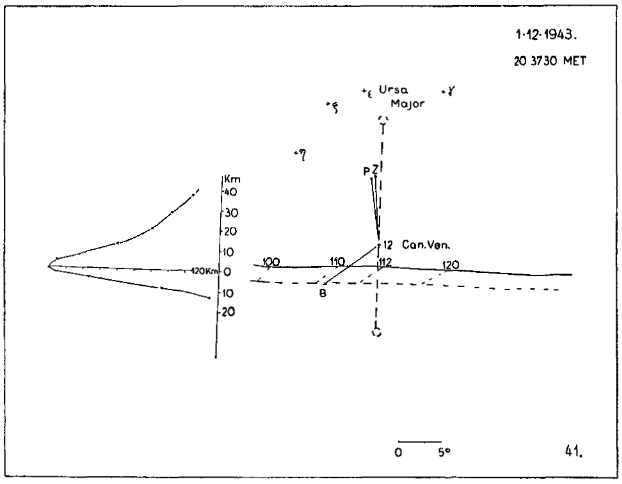
1·12·1943.
20 37.30 MET
Ursa
Major
Km
40
30
20
10
0
10
20
120Km
P
Z
12
Can.Ven.
100
110
112
120
B
0 5°
41.

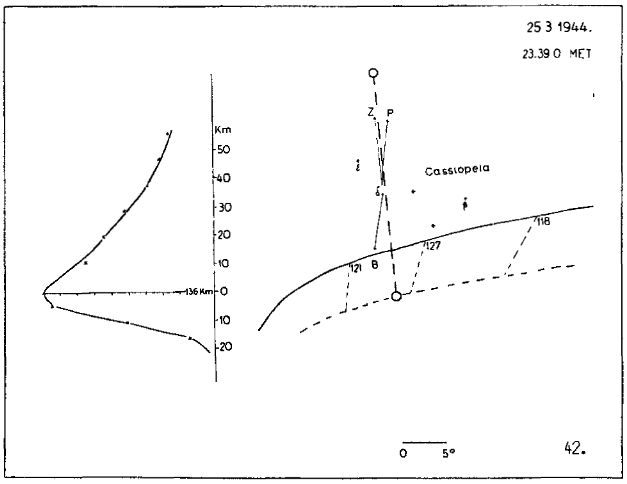
25 3 1944.
23.39.0 MET
Km
50
40
30
20
10
0
10
20
136Km
Z
P
Cassiopeia
118
127
121
B
0 5°
42.

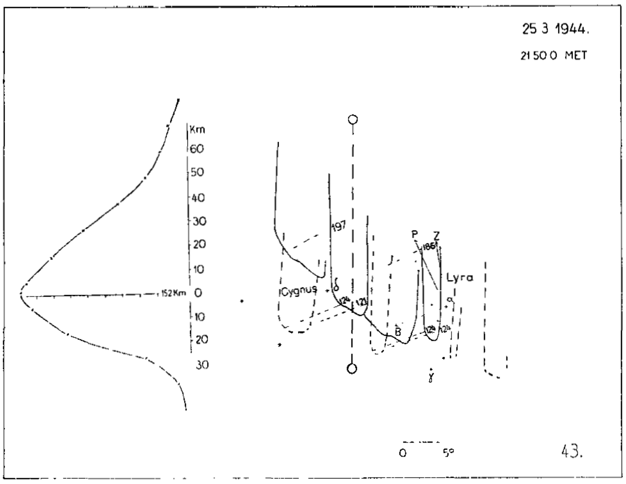
25 3 1944.
21 50 0 MET
Km
152 Km
Cygnus
Lyra
0 5°
43.

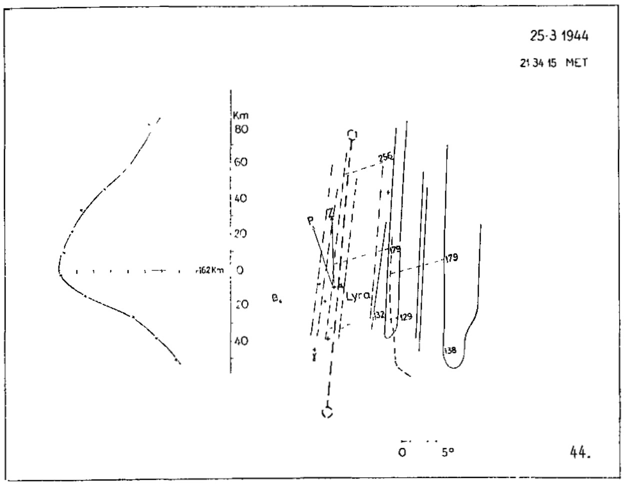
25·3 1944
21 34 15 MET
Km
162 Km
Lyra
0 5°
44.

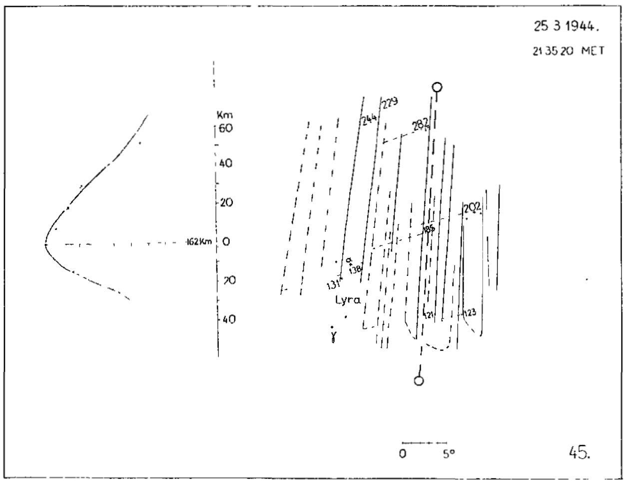
25 3 1944.
21 35 20 MET
Km
162 Km
Lyra
0 5°
45.

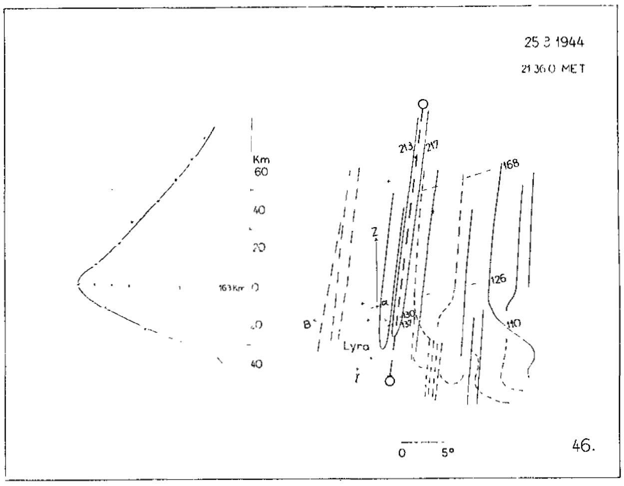
25 3 1944
21 36 0 MET
Km
Lyra
0 5°
46.

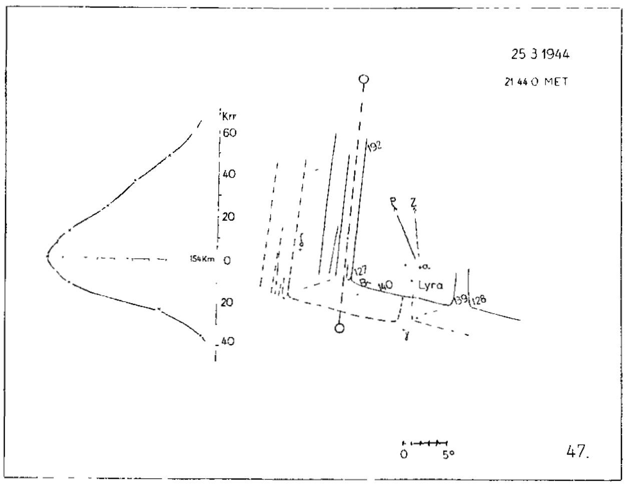
25 3 1944
21 44 0 MET
154 Km
Lyra
0 5°
47.

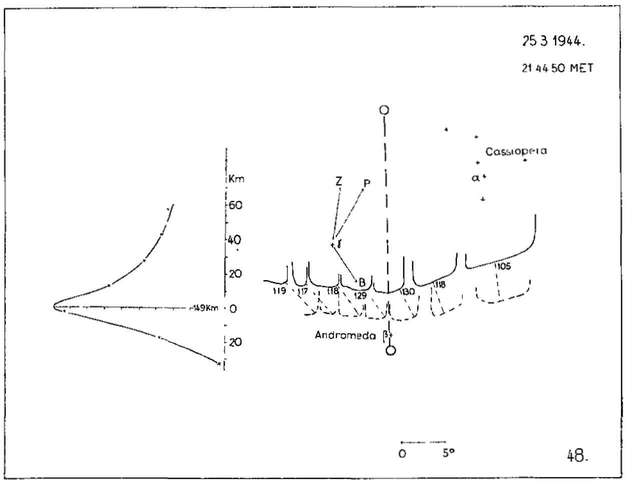
25 3 1944.
21 44 50 MET
Cassiopeia
Km
149 Km
Andromeda
0 5°
48.

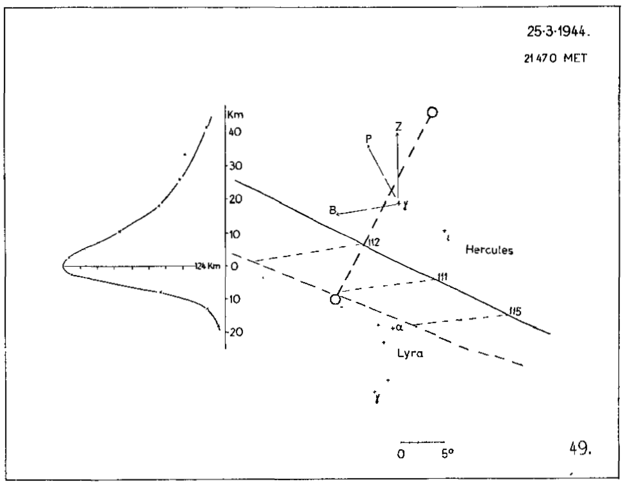

49.

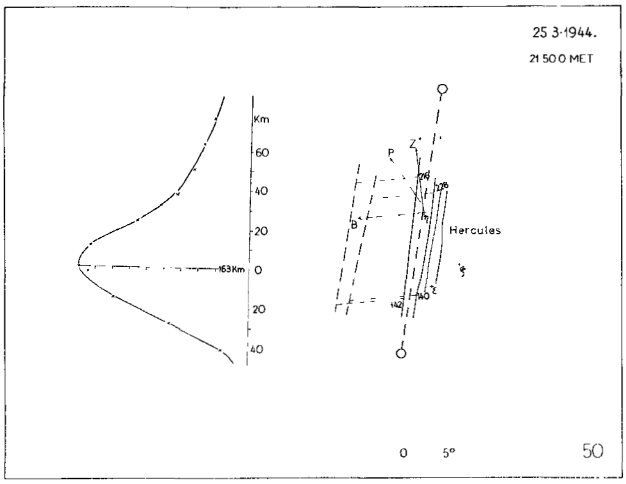

50

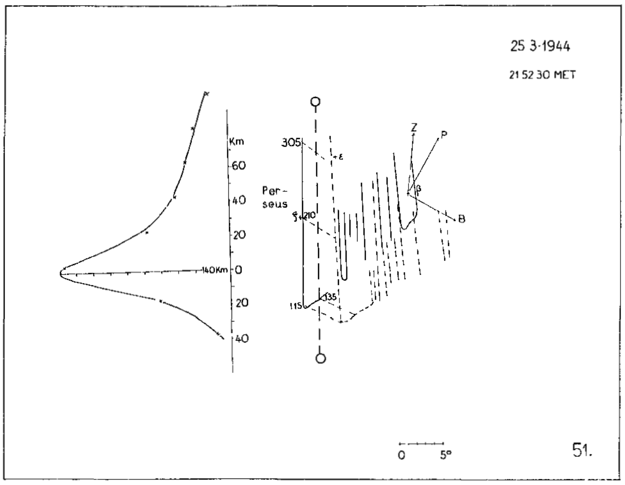

51.

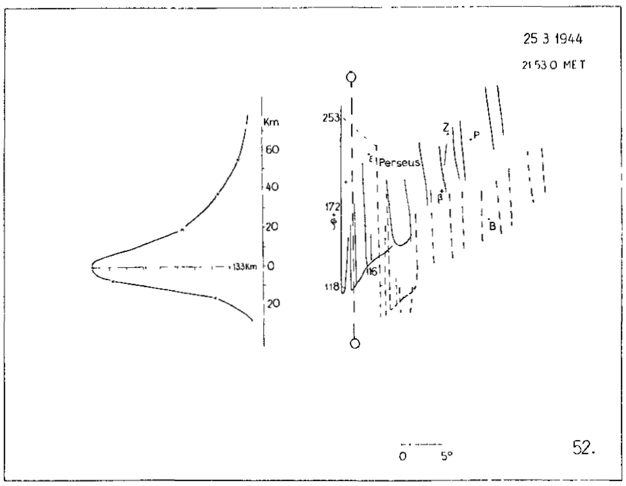

52.

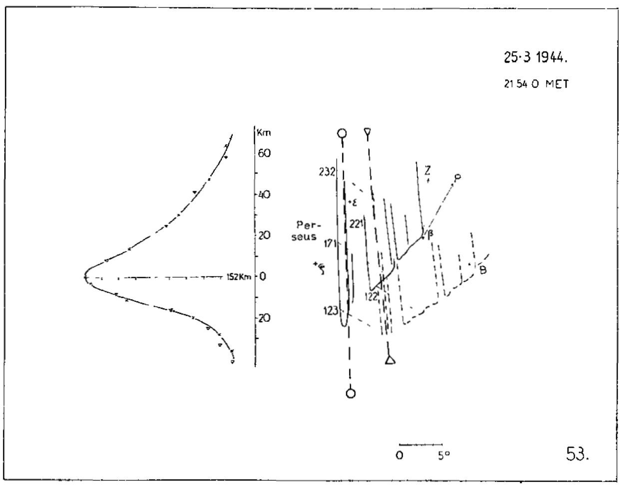

53.

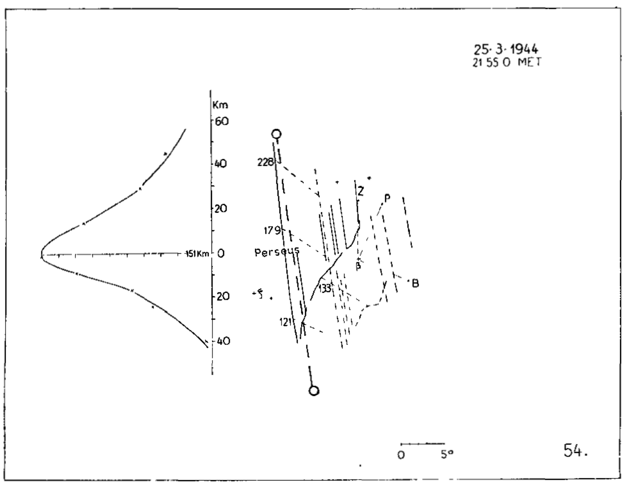

54.